

ANKARA UNIVERSITY

INSTITUTE OF NUCLEAR SCIENCES

MASTER'S THESIS

**THE EFFECT OF THE USE OF THERMOPLASTIC MASK
ON SKIN DOSE
IN HEAD AND NECK IRRADIATION**

ELÇİN İLKE OKUR

DEPARTMENT OF MEDICAL PHYSICS

HEALTH PHYSICS MASTER'S PROGRAM

ANKARA

2019

All Rights Reserved

THESIS APPROVAL

The thesis entitled “The Effect of the Thermoplastic Mask on Skin Dose in Head and Neck Irradiation” prepared by Elçin İlke OKUR in partial fulfillment of the requirements for the degree of Master of Science in Health Physics Program of the Medical Physics Department of Institute of Nuclear Sciences in Ankara University has been examined and approved by the undersigned jury members.

Advisor: Prof. Dr. Şaban Çakır GÖKÇE

Co-Advisor: Assoc. Prof. Dr. Gaye Özgür ÇAKAL

Jury Members:

Prof. Dr. Şaban Çakır GÖKÇE
Ankara University Faculty of Medicine Radiation Oncology Department



Assoc. Prof. Dr. Gaye Özgür ÇAKAL
Ankara University Institute of Nuclear Sciences



Prof. Dr. Ali Ulvi YILMAZER
Ankara University Faculty of Engineering Physics Engineering Department




Prof. Dr. Ayşe HIÇSÖNMEZ
University of Yüksek İhtisas Radiation Oncology Department

Assoc. Prof. Dr. TURAN OLGAR
Ankara University Faculty of Engineering Physics Engineering Department



Approved



Prof. Dr. Niyazi MERİÇ
Head of the Institute of Nuclear Sciences

I hereby declare that all information in this thesis has been obtained and presented in accordance with academic rules and ethical conduct. I also declare that, as required by these rules and conduct, I have fully cited and referenced all material and results that are not original to this work.

Name, Last Name: Elçin İlke OKUR

Signature :

A handwritten signature in blue ink, appearing to read 'Elçin İlke OKUR', written in a cursive style.

ABSTRACT

Master's Thesis

THE EFFECT OF THE USE OF THERMOPLASTIC MASK ON SKIN DOSE IN HEAD AND NECK IRRADIATION

Elçin İlke OKUR

Ankara University Institute of Nuclear Sciences

Department of Medical Physics

Health Physics Master's Degree Program

Supervisor: Prof. Dr. Şaban Çakır GÖKÇE

Co-Supervisor: Assoc. Prof. Dr. Gaye Özgür ÇAKAL

Thermoplastic masks used for immobilization in radiotherapy cause the skin to take extra doses due to scattering during irradiation. This study aims to measure the effect of the use of thermoplastic masks on skin doses. In vivo skin dose measurements were compared with treatment planning system (TPS) calculations in this study.

Masks were applied to ten patients who decided to take radiotherapy on their head and neck region. Their computerized tomography (CT) images with 2.5 millimeter (mm) cross sections were taken. Treatment plans of the patients were created in intensity modulated radiotherapy (IMRT) technique. At the beginning of the treatment, the masks were marked and TLD were placed under the mask for in vivo measurements. TLD were irradiated in vivo, during the treatment.

Following the TLD reading procedure, the measured daily doses were compared with the daily doses calculated by TPS. The difference was evaluated as the effect of the thermoplastic mask. According to the results, the average daily dose calculated by the planning system was 134.6 centi-gray (cGy) while the averaged daily dose measured by TLD was 151.4 cGy. The average difference of 16.8 cGy, which was not calculated by the planning system, corresponded to a percentage of 12.6%. The difference between the calculations and measurements ranged from 0.1% to 29.3%. The difference was found to be statistically significant ($p < 0.001$).

2019, 69 pages

Keywords: Radiotherapy, head and neck radiotherapy, skin dose, thermoplastic mask

ÖZET

Yüksek Lisans Tezi

BAŞ VE BOYUN IŞINLAMALARINDA TERMOPLASTİK MASKE KULLANIMININ CİLT DOZUNA ETKİSİ

Elçin İlke OKUR

Ankara Üniversitesi Nükleer Bilimler Enstitüsü

Medikal Fizik Anabilim Dalı

Sağlık Fiziği Yüksek Lisans Programı

Danışmanı: Prof. Dr. Şaban Çakır GÖKÇE

Eş-Danışmanı: Doç. Dr. Gaye Özgür ÇAKAL

Radyoterapide immobilizasyon amacı ile kullanılan termoplastik maskeler radyoterapi sırasında saçılma nedeni ile cildin fazladan doz almasına neden olmaktadır. Bu tezde, termoplastik maskelerin cilt dozuna olan etkisi incelenmiştir. İnceleme hastalardan alınan in vivo ölçümlerin sonuçları ile tedavi planlama sisteminde (TPS) hesaplanan dozların karşılaştırılması ile yapılmıştır.

Baş boyun radyoterapisi alacak olan on hastaya maskeler uygulanmış ve 2.5 milimetre (mm) aralıklı kesitlerle bilgisayarlı tomografi görüntüleri alınmıştır. Hasta planları yoğunluk ayarlı radyoterapi tekniği ile hazırlanmıştır. Hasta tedavi alacağı zaman, termoplastik maskeler işaretlenmiş ve maskerin iç yüzeyine termoluminesans dozimetreler (TLD) yerleştirilmiştir. TLD, in vivo olarak tedavi sırasında ışınlanmıştır.

TLD okuma işlemlerinden sonra sonuçlar TPS tarafından hesaplanan dozlarla karşılaştırılmıştır. TPS ile in vivo ölçüm arasındaki fark maskenin etkisi olarak değerlendirilmiştir. Elde edilen sonuçlar değerlendirildiğinde TPS tarafından hesaplanan günlük dozların ortalaması 134.6 santi-gray (cGy), TLD ile ölçülen günlük dozların ortalaması ise 151.4 cGy bulunmuştur. Aradaki 16.8 cGy farkın miktarı yüzde olarak 12.6%'dır. Ölçüm sonuçları ile planlama sistemi hesaplamaları arasındaki fark 0.1% ile 29.3% arasında değişmektedir. Aradaki fark istatistiksel olarak anlamlı bulunmuştur ($p<0.001$).

2019, 69 sayfa

Anahtar Kelimeler: Radyoterapi, baş ve boyun radyoterapisi, cilt dozu, termoplastik maske

ACKNOWLEDGMENTS

Firstly, I would like to thank my advisor, Dear Prof. Dr. Şaban Çakır Gökçe, who gave me the honour to be his student in the Ankara University Faculty of Medicine Radiation Oncology Department. I offer my sincerest gratitude to him for his continuous support, patience and motivation during my master's thesis. I would like to thank my co-advisor Dear Assoc. Prof. Dr. Gaye Özgür Çakal for her sincere suggestions for preparing this thesis. I feel so lucky to have her as a mentor who guided me with her knowledge and experiences. I appreciate her warm heartedness, kindness and support. I would like to thank Dear Prof. Dr. Niyazi Meriç, who provided me with the technical infrastructure at the Ankara University Institute of Nuclear Sciences during my studies. I would like to thank Dear Prof. Dr. Ayşe Hiçsönmez, who has made a great contribution to the radiation oncology physics and directed me to this field. I would like to offer my gratitude to Dear Prof. Dr. Haluk Yücel for his guidance during my studies. I would like to thank Dear Assoc. Prof Dr. George S. Polymeris for encouraging me during all the studies at the Institute of Nuclear Sciences. Also, I would like to thank medical physicists Dear Tuğba Atakul, Dear Ayfer Temür and Dear Yakup Arslan, and the radiation oncology specialists Dr. Tuğçe Kütük and Dr. Esra Gümüştepe at Ankara University Faculty of Medicine Radiation Oncology Department for all their help and guidance. I am also grateful to the technicians of the Ankara University Radiation Oncology Clinique; Kayahan Kuzucu, Yeliz Karakoç, Hakan Günay and Şüheda Ercan for their help during in vivo measurements. Additionally, and especially I would like to thank the technicians Dear Ümit Can Çetinkaya and Mehmet Furkan Mert for their help during photographing. I would like to thank my dear friends and Research Assistants Dear Engin Aşlar and Dear İbrahim Demirel for the share of their knowledge, experience and recommendation.

Above all, I am very grateful for the endless love and support of my dear parents, my father Ferruh Okur and my mother Deniz Okur. I feel stronger and happier with their love and support.

TABLE OF CONTENTS

ABSTRACT	i
ÖZET.....	ii
ACKNOWLEDGMENTS	iii
TABLE OF CONTENTS.....	iv
LIST OF SYMBOLS AND ABBREVIATIONS	viii
TABLE OF FIGURES.....	ix
TABLE OF TABLES.....	x
1. INTRODUCTION.....	1
2. THEORY	3
2.1 Head and Neck Cancers	3
2.1.1 Epidemiology of head and neck cancers	3
2.1.2 Etiology and risk factors.....	3
2.2 Head and Neck Anatomy	4
2.3 Types of Head and Neck Cancers	5
2.3.1 Nasopharynx cancers	5
2.3.2 Nasal cavity and paranasal cancers.....	6
2.3.3 Orbital cancers	6
2.3.4 Oral cavity cancers.....	7
2.3.5 Oropharynx cancers.....	7
2.3.6 Hypopharynx and cervical esophagus cancers.....	7

2.3.7 Larynx cancers	8
2.3.8 Thyroid and parathyroid cancers.....	8
2.3.9 Salivary gland cancers	8
2.4 Treatment Options for Head and Neck Cancers.....	9
2.4.1 Surgery	9
2.4.2 Chemotherapy	9
2.4.3 Radiotherapy	10
2.5 External Radiotherapy Techniques in Head and Neck Cancers	10
2.5.1 Conventional two dimensional radiotherapy technique.....	11
2.5.2 Three dimensional conformal radiotherapy (3DCRT) technique	11
2.5.3 Intensity modulated radiotherapy (IMRT) technique.....	11
2.6 Skin.....	14
2.6.1 Skin layers.....	14
2.6.2 Skin doses.....	14
2.7 Immobilization Systems for Head and Neck Radiotherapy	15
2.7.1 Head and neck support pillows.....	16
2.7.2 Thermoplastic masks	16
2.8 Quality Assurance in Radiotherapy	18
2.8.1 In vitro dosimetry and phantoms	18
2.8.2 In vivo dosimetry in external radiotherapy and dosimeters	19
2.9 Thermoluminescence Dosimetry	22

2.9.1 Luminescence mechanism	22
2.9.2 Thermoluminescence measurement	23
2.10 Studies Related to the Skin Dose Estimations and Use of Thermoplastic Masks.....	25
3. MATERIAL AND METHOD.....	29
3.1 Material.....	30
3.1.1 Patients	30
3.1.2 GE Optima 580 RT computerized tomography device	30
3.1.3 Thermoplastic mask.....	31
3.1.4 CT marker	32
3.1.5 Eclipse TPS	33
3.1.6 Varian Clinac DHX linear accelerator.....	34
3.1.7 TLD chips.....	35
3.1.8 Solid water phantoms	36
3.1.9 PTW -TLDO TLD annealing oven	36
3.1.10 Harshaw TLD model 3500 manual reader	38
3.2 Method	39
3.2.1 Planning system calculations.....	39
3.2.1.1 Preparation of patients for the treatment.....	39
3.2.1.2 Determination of the points that will be measured from TPS	41
3.2.2 In vivo skin dose measurements	44

3.2.2.1 TLD preparation for usage	45
3.2.2.2 Determination of points to be measured	47
3.2.3 Comparison of calculated doses with measured doses	50
3.2.4 Statistical analysis	50
4. RESULTS	51
5. DISCUSSION	59
6. CONCLUSION AND RECOMMENDATION	63
REFERENCES	65
CURRICULUM VITAE.....	69

LIST OF SYMBOLS AND ABBREVIATIONS

C°	Celcius Degree
cGy	Centi Gray
cm	Centi Meter
CT	Computerized tomography
CB	Conduction Band
°	Degree
ECC	Electric Correction Coefficient
EPID	Electronic Portal Imaging Device
Gy	Gray
HPV	Human Papilloma Virus
KERMA	Kinetic Energy Released in Matter
IMRT	Intensity Modulated Radiortherapy
ICRU	International Commission of Radiation Units
LiF	Lithium Fluoride
Mg	Magnesium
MOSFET	Metal Oxide Semiconductor Field Effect Transistors
mm	Millimeter
MeV	Million Electron Volt
MV	Million Volt
MLC	Multi Leaf Collimator
OSL	Optically Stimulated Dosimeters
RCF	Reader Calibration Factor
s	Second
SCC	Squamous Cell Carcinomas
TLD	Thermoluminescence Dosimeters
3DCRT	Three Dimensional Conformal Radiotherapy
Tl	Tallium
TPS	Treatment Planning Systems
VB	Valence Band

TABLE OF FIGURES

Figure 2.1 Simple Head and Neck Anatomy	4
Figure 2.2 Contoured Critical Structures and Target Volumes on CT Images.....	12
Figure 2.3 Beam Selection For the Tumor.....	13
Figure 2.4 Plot of Absorbed Dose and Kinetic Energy Released in Matter	15
Figure 2.5 Head and Neck Support Pillows	16
Figure 2.6 Thermoplastic Masks.....	17
Figure 2.7 Thermoplastic Mask Inside a Bath	17
Figure 2.8 Diode MOSFET and EPID Dosimeters	20
Figure 2.9 Gel, Radiochromic, OSL Dosimeters	21
Figure 2.10 Fluorescence and Phosphorescence Mechanism	23
Figure 2.11 Schematic Diagram of a TLD Reader	24
Figure 2.12 Glow-Curve of LiF	24
Figure 3.1 GE Optima 580 RT Computed Tomography Device	31
Figure 3.2 Thermoplastic Mask Application	32
Figure 3.3 Different Views of a CT Marker	33
Figure 3.4 Planning Interface of TPS	34
Figure 3.5 Varian DHX Linear Accelerator.....	35
Figure 3.6 TLD Chips	36
Figure 3.7 Solid Water Phantoms in Different Thicknesses	36
Figure 3.8 PTW- TLDO Annealing Oven.....	37
Figure 3.9 Stainless Steel Annealing Tray	38
Figure 3.10 Harshaw TLD 3500 Manual Reader.....	39
Figure 3.11 Preparation of Thermoplastic Mask for Patient.....	40
Figure 3.12 Patient's Being Prepared to Take Tomography Images.....	40
Figure 3.13 Critical and Target Volumes	41
Figure 3.14 Four Anterior Angled Beams were Selected for Each Patient	42
Figure 3.15 A Schematic Diagram Showing Gantry Angles Choosed	42
Figure 3.16 Determination of the Calculated Doses at Marked Points.....	43
Figure 3.17 The Body Contour and 2 mm Reference Contour	44
Figure 3.18 Patient Positioning and Gantry Rotation	45
Figure 3.19 Setup for TLD Calibration Irradiation.....	46
Figure 3.20 Marking the Masks for TLD Location	48
Figure 3.21 Thermoplastic Mask Marked.....	49
Figure 4.1 Mean of Calculated and Measured Skin Dose Values.....	58

TABLE OF TABLES

Table 3.1 Patient Information	30
Table 4.1 Treatment Plan Data of the Patients.....	51
Table 4.2 Calculated Doses of Determined Volumes	52
Table 4.3 Measurement Results of TLD Located Under the Mask	54
Table 4.4 Comparison of Measured and Calculated Doses	56
Table 4.5 Paired Sample Test Statistics	57



1. INTRODUCTION

Head and neck cancers are the ninth most common cancer constituting 4% of all cancer types and causes 1.2% death among all cancer types (Gunderson and Tepper 2016, Gupta et al. 2016). In Turkey, head and neck cancers are the seventh most common cancer type. Factors such as smoking, using alcohol, chewing tobacco, bad diet habits and long-term exposure to sunlight increase the head and neck cancer incidence. Head and neck cancers are one of the most curable malignities when diagnosed at early stages (<http://kanser.gov.tr/index.php/kanser/kanser-turleri/774-ba%C5%9F-ve-boyun-kanserleri> 2018).

Surgery, radiotherapy and chemotherapy can be counted as the treatments for head and neck cancer. Radiotherapy and surgery are the main treatment options for most of the time. Chemotherapy is an adjuvant for the other treatment options. Head and neck region is a complex part of the body including the beginning of the digestion and respiratory system, main veins, all neurons and sense organs of the body being in a very narrow area. Surgery may not be easy in such a complex area. In such cases radiotherapy may become the main treatment choice (Ki-Oh et al. 2016).

Radiotherapy is one of the most common techniques for cancer treatments. Radiotherapy techniques are improved especially in recent years. In radiotherapy mainly, the cancer cells are destroyed by high-energy electromagnetic radiation or high energetic particle radiation.

Intensity modulated radiotherapy (IMRT) is a radiotherapy technique relatively protecting the environmental tissues while irradiating the tumor volume. Although the technique relatively protects the environmental tissues, it is not possible not to damage any tissue other than tumor volume. Incoming radiation to the body is absorbed in all the tissues it passed through. Thus, these environmental tissue doses should be calculated correctly by the treatment planning systems (TPS). Although the planning systems calculate dose distributions very similar to real doses at critical organs and tumor volume, they fail at entrance doses. This results in miscalculated skin doses. In head and neck cancers, some immobilization systems are being used to prevent the undesired movements of patients. Thermoplastic masks are one of the most common immobilizing devices for head and neck region. They are molded individually for each patient before

his or her treatment. However, according to their composition and thicknesses, these masks cause an increase in skin doses. The excess skin doses cause dermatological problems and this is an undesirable situation especially in head and neck regions. When the masks are applied to patients, these masks are detected as entrance material, by planning systems. Thus, the scatterings due to thermoplastic material and the backscattering doses cannot be calculated correctly. Therefore, the real skin doses should be verified with ways that are more trustable.

In vivo measurement may be a solution for correct skin doses. In vivo measurement is direct detection of the radiation from the body. To predict the skin reactions according to absorbed radiation dose and choose the best adjuvant support for skin, the effect of the mask should be known and real skin doses should be measured. In order to measure the doses, electronic portal imaging devices (EPID), diodes, luminescence dosimeters are mainly used.

This study aims to observe the differences between the doses calculated by TPS and in vivo doses of the patients measured by using thermoluminescence dosimeters (TLD) during the treatment and to observe the effect of the thermoplastic masks.

2. THEORY

2.1 Head and Neck Cancers

Head and neck cancers usually start from squamous cell and named as squamous cell carcinomas (SCCs). SCCs constitute 90 % of the head and neck cancers (Sanderson and Ironside 2002).

Head and neck cancers can also be named according to their location. Oral cavity cancers, salivary gland cancers, paranasal sinuses and nasal cavity cancers, nasopharyngeal- oropharyngeal - hypopharyngeal cancers, larynx and upper neck cancers are named as head and neck carcinomas (Engin and Erişen 2003).

2.1.1 Epidemiology of head and neck cancers

Head and neck cancers are ninth most common cancer type in the world. 685,000 new cases are recorded annually. It has high mortality rates in developing countries, up to two third in five years. Head and neck carcinoma incidence is higher in male than female (Gupta et al. 2016).

The most common type of the head and neck cancer in male is oral cavity and larynx cancers, the most common type of the head and neck cancer in women is oropharyngeal and pharyngeal cancers, worldwide. However, in Turkey in both male and female the most common type of head and neck cancers are oral cavity and larynx cancers (Engin and Erişen 2003).

2.1.2 Etiology and risk factors

Smoking cigarettes, pipe and cigar (for both smoker and the passive smoker), drinking alcohol, having human papilloma virus (HPV) and Epstein Barr virus can be counted in typical risk factors.

Genetic susceptibility, nutritional deficiencies, vitamin deficiencies, poor oral hygiene, inappropriate prosthesis use, chronic infections are other risk factors leading to the development of head and neck cancer. Because of higher exposure to causative agents in males, like tobacco and alcohol, incidence increases after 50 years old (Gupta et al. 2016).

2.2 Head and Neck Anatomy

Head and neck region can be divided into six-sub region. Nasal cavity, pharynx, larynx, oral cavity, oropharynx and hypopharynx cancers (Lester and Young 2012). A simple schematic diagram of head and neck anatomy is given in the Figure 2.1.

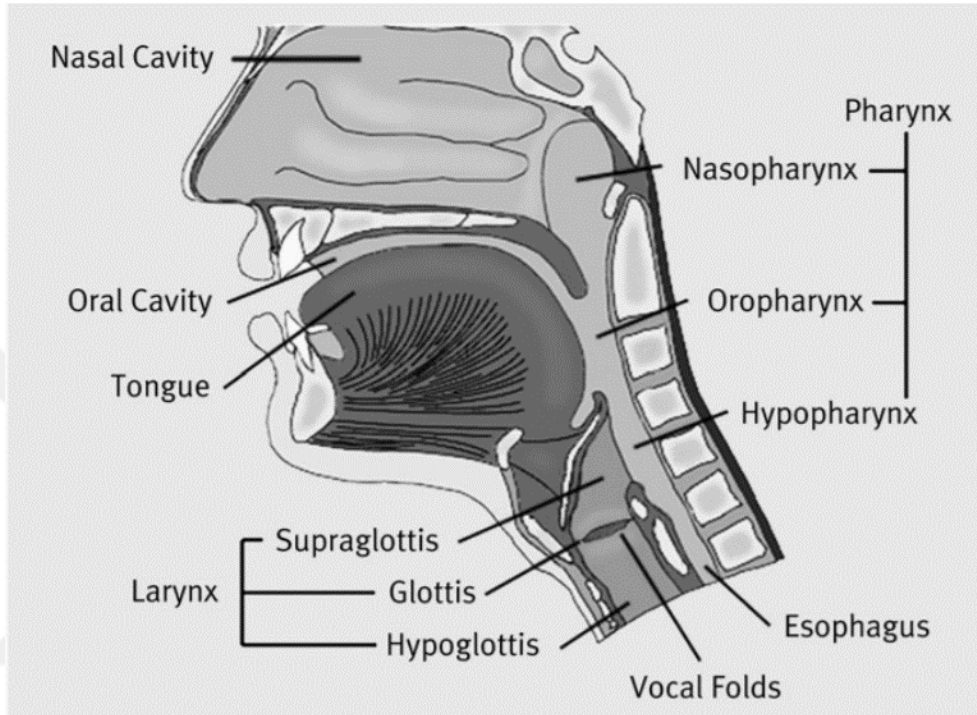


Figure 2.1 Simple Head and Neck Anatomy (Lester and Young 2012)

Oral cavity includes lips, two third of the tongue, floor of the mouth, retromolar trigon, mandibula, alveolar surfaces of maxilla bones, buccal mucosa and hard palate. The Sino nasal region consists of the nasal vestibule, nasal cavity, maxillary, ethmoid, frontal, and sphenoid sinuses. The nasal vestibule is the area that remains inside the nose wings. The nasal cavity is located at the bottom of the area from the top to the base of the skull. The lateral walls form the medial wall of the maxillary sinus and are divided into right and left by the nasal septum. Oropharynx consists of soft palate, bed of tonsil, and tonsils, tongue base, nasopharynx and side pharyngeal walls between epiglottic folds. Hypopharynx consists of bilateral pyriform sinuses, pharynx walls, post cricoid region and cervical esophagus. It starts from oropharynx limited with hyoid bone from above, lays until the cervical esophagus in the height of cricoid cartilage. Larynx is divided into

three sub regions anatomically. Glottic larynx where the vocal folds are located, the supraglottic larynx above the vocal folds and the subglottic larynx under the vocal folds. Vocal folds and frontal commissure are located in glottic larynx. Subglottic larynx includes pseudocords, epiglottis, arytenoid cartilage and aryepiglottic folds. Thyroid is a butterfly shaped organ in front of the second and third circle of the trachea cartilage. It has 2 lobes, each 3-4 cm long, 2 cm width and 3-4 millimeter (mm) thick (Çetingoz 2013).

2.3 Types of Head and Neck Cancers

2.3.1 Nasopharynx cancers

Nasopharynx cancer is the only cancer type that has the first treatment choice of radiotherapy. The other head and neck cancers in early stages can be treated with surgery, chemotherapy or radiotherapy, but the only choice for nasopharynx carcinomas is radiotherapy. Adjuvant chemotherapy may be a supportive treatment choice. While nasopharynx cancer is common on southern-east Asian countries, it is rare at European countries. Although the disease is observed after middle ages, in Turkey it is common at the ages between 10 - 30. Nasopharynx cancers are more sensitive to radiation than the others. This increases the importance of protecting the healthy tissue for late effects of radiation. At the early stages, the treatment success rates for the cure reaches at 80-95%. Even at late stages, the cure rate is about 40-70%. Epstein Barr Virus and genetic susceptibility is a suspicious agent for nasopharynx cancer (Çetingoz 2013).

Different side effects due to radiation treatment can be observed in several intensities. Early stage side effects are observed during radiotherapy and after a few weeks. Radiation mucositis affecting oral mucosa shows itself in early stages of radiotherapy in the form of sore throat and difficulty in swallowing. In subsequent fractions, the complaints like rash, dry desquamation followed by water desquamation increases. Although these complaints are relieved with given medicines they are not expected to heal completely. It should be known that early side effects, usually occur around the 10th fraction after the treatment starts. For this reason, there may be different reasons for disturbances that occur earlier (Çetingoz 2013).

Late side effects in the head and neck region can cause very serious permanent problems. In particular, the unplanned overdose of the spinal cord may result in permanent paralysis. In addition to hearing loss, cosmetic problems such as fibrosis, telangiectasis, color changes in the neck skin may also be seen. In addition, radiation-induced secondary tumors can also be observed over the years in other areas of the site (Çetingoz 2013).

2.3.2 Nasal cavity and paranasal cancers

Nasal cavity and paranasal sinuses tumors are rarely observed. Wood dust, synthetic wood glues, chromium, radium and isopropyl alcohol increases the incidence.

Even if the primary treatment option is surgery, radiotherapy is the most preferred treatment option because the surgical boundaries is less likely to be negative. Better cosmetic results is another reason to prefer radiotherapy. Local control is good at early stages (Engin and Erişen 2003, Çetingoz 2013).

Side effects due to radiation treatment include otitis, ringing in the ears and hearing problems. Influence of the pituitary gland may cause endocrine dysfunction. Attachments may occur in the nasal cavity (Çetingoz 2013).

2.3.3 Orbital cancers

Orbital tumors are rarely observed. The most encountered ones are melanomas. Exposure to sunlight, immunosuppression and having light color iris increases the incidence in basal cell carcinoma and squamous cell carcinoma. Ocular structures consist of eyelids, eyelashes, cilia, lacrimal glands, drainage systems, and conjunctiva. The most observed type of cancer in this region is not SCC it is basal cell carcinoma. Surgery is preferred for eyelid and surrounding cancers but radiotherapy is very advantageous because it protects the eyeball and visual function.

As a side effect due to radiotherapy, erythema hyperpigmentation, depigmentation, atrophy and telangiectasia can be seen. Eyebrows, eyelashes, hair in the area can be poured. Radiation-induced cataract is the most important side effect and can be easily treated with surgery (Çetingoz 2013).

2.3.4 Oral cavity cancers

Oral cavity cancers account for 30% of all head and neck cancers and they are the most common type of the head and neck cancers. It is mostly observed on older ages and males. Use of tobacco and alcohol is responsible from these cancers. The aim of the treatment of oral cavity cancers is to cure and protect the functions as much as possible and complete the treatment with the possible least side effects. Radiotherapy and surgery is the main treatment options while chemotherapy is an adjuvant therapy option to them (Çetingoz 2013).

Acute mucositis, tasting disorders, low salivation are early radiotherapy side effects. The late side effects of radiotherapy are mouth instability, tooth decay, trichism, and rarely soft tissue necrosis (Engin and Erişen 2003).

2.3.5 Oropharynx cancers

Oropharynx cancers account for 0.5 % of all cancers. Surgery is the first treatment option. While radiotherapy is the adjuvant treatment choice, hybrid of radiotherapy with surgery is the most proper treatment option. The chemotherapy is adjuvant to radiotherapy or it is the main treatment for late stage in inoperable tumors (Çetingoz 2013).

Mucositis and dysphagia are important side effects observed due to radiotherapy. Side effects such as laryngeal edema, fibrosis, hearing loss and trismus may also be seen (Engin and Erişen 2003).

2.3.6 Hypopharynx and cervical esophagus cancers

Hypopharynx and cervical esophagus has a role on swallow functions. Studies show that use of tobacco and alcohol are important risk factors for cancers at this area. They account for less than 6% of all head and neck tumors. According to patient's age, sex, life and diet habits, social and profession life and clinical status, radiotherapy or surgery might be the primary treatment option in early stages. However, the location of the hypopharynx is not so proper for surgery due to its high probability of postoperative morbidity. Late stages are not even proper for surgery. Thus, radiotherapy is the most preferred treatment option. Chemotherapy is necessary for an adjuvant treatment option (Çetingoz 2013). At this region, normal tissue is an important limiter. Especially 45 Gy for any point of spinal cord

and 60 Gy for any point of brachial plexus should not be reached. Due to the side effects of radiotherapy, additional food support may be required (Engin and Erişen 2003).

2.3.7 Larynx cancers

Larynx cancers are the second most common cancers in head and neck carcinomas. Males have a four times more incidence relative to females. Age, sex, use of tobacco and alcohol, genetical factors, weakness at immune system are the risk factors. While tobacco use increases the risk 2.5 to 20 times, alcohol use increases the risk 2 to 5 times. Use of both of them increases the risk 50 to 100 times. The incidence is higher at males after ages of 55. Main aim of the treatment is to cure. At early stages only one treatment is preferred, mostly radiotherapy to protect the voice and speaking function. Hybrid of two treatment option is suggested for late stage tumors (Engin and Erişen 2003).

Radiotherapy increases difficulty of speaking, dysphagia, mucositis, skin rashes darkening and peeling and weight loss. Acute side effects calm down and disappear after about a month. There may be taste dysfunction and permanent mouth instability. As a late radiation complication, jaw edema and laryngeal edema may occur (Engin and Erişen 2003, Çetingoz 2013).

Larynx cancers often recur within the first three years, and therefore periodic controls are very important (Engin and Erişen 2003).

2.3.8 Thyroid and parathyroid cancers

Thyroid cancers account for 2% of all the cancer types. Even if thyroid tumor is being observed in 7% of the population, only 4% to 6.5% of them are malign. This is the most common endocrinal malignity and it consist of 95% of endocrine malignities. It is common in female but more fatal in male. Age, sex, family history, genetical factors and exposure to ionizing radiation can be counted as risk factors. The main treatment option is surgery (Engin and Erişen 2003, Çetingoz 2013).

2.3.9 Salivary gland cancers

Salivary glands are parotid glands, submandibular glands and sublingual glands. They are one of the rare cancer types observed in head and neck region. 80% of salivary gland

cancers are based on parotid glands. While 15% of them are caused by submandibular glands, the rest, 5% are caused by sublingual glands. Use of tobacco and alcohol, genetic factors, being a coiffeur, exposure to plastic and metal-nickel industry, and exposure to ionizing radiation can be counted as probable risk factors. Nevertheless, a significant factor could not find. Primary treatment option is surgery. Adjuvant radiotherapy decreases the rates of spreads and recurrences. Chemotherapy is limited with metastatic tumors (Çetingoz 2013).

2.4 Treatment Options for Head and Neck Cancers

Because of the complexity of this region, multidisciplinary treatment is applied. As mentioned above, there are three main approaches for head and neck carcinomas. While surgery or radiotherapy may be the only treatment option for stages I or II, different combinations of those approaches are applied together for stages III and IV cancers (Tariq et al. 2015). In this part general information about treatment options approaches is given.

2.4.1 Surgery

The primary treatment option for head and neck cancers is surgery except nasopharynx region. Frequently located lymphatic nodes at head and neck region hardens and widens the treatment area according to the stage of the tumor and metastasis. Lymphatic drainage gains importance for the management of the disease. However, it is hard to get negative surgical margins with surgery while protecting the functions like speaking, swallowing etc. As positive surgical margins are associated with decreased survival rates, an adjuvant therapy is required for those margins. Besides, showing same prognoses with radiotherapy causes the surgery to remain as the secondary option (Galbiatti et al. 2013).

2.4.2 Chemotherapy

It has been shown that platinum-based chemotherapy (cisplatin) makes tissue more radiosensitive. Consequently, radiotherapy effectiveness increases. This much effective treatment is preferable for advanced stage tumors. Chemotherapy may be a palliative treatment option for advanced stage tumors (Gunderson and Tepper 2016).

2.4.3 Radiotherapy

It is shown that, although radiotherapy is not the primary option for treatment choice, it gives the similar prognosis with surgery, while protecting the functions like speaking, swallowing, and using mimics. Protecting functions and good prognosis and necessity of adjuvant therapy in the case of surgery with negative margins, increases the importance of radiotherapy. Besides this radiotherapy can be applied as pre-operative or post-operative on the patient (Çetingoz 2013). Applying radiotherapy with adjuvant chemotherapy gives good results on palliative disease.

A typical external radiation treatment for head and neck region is about 65 Gy with about 2 Gy daily dose. It takes average 6 or 7 weeks to complete the whole treatment. In order to irradiate the tumor with prescribed dose and minimize the dose to environmental healthy organs, movement of the patient should be as small as possible. Especially narrowity at this region and the closeness of the organs to each other increases the importance of movements. As a precaution to limit the movement of the patient and ease to lay the patient, the thermoplastic masks are produced for head and neck tumors (Lee et al. 2002).

2.5 External Radiotherapy Techniques in Head and Neck Cancers

As the necessity for radiation treatment is increased, the treatment techniques are improved rapidly. Today, radiation treatment can be given to the patient in two ways. In internal radiotherapy, the radiation sources are directly placed in tumor or cavities close to tumor. This method is named as brachytherapy and it requires special devices including radiation sources, different from devices using in external radiotherapy. As the maximum dose homogeneities are obtained for the tumor and healthy tissue sparing effects of placing radioactive sources directly in the tumor are considered, it can be said that brachytherapy is the most proper method for the radiotherapy (Gunderson and Tepper 2016). However, the long treatment sessions and special devices may not be proper for busy cliniques.

The second method is external radiotherapy, in which the radiation is applied to the patient externally. External radiation can be given in the form of particle radiation or electromagnetic radiation. When the particular radiation is going to be applied, the

particles are accelerated through medical linear accelerators, and heavy structures are produced for external radiotherapy applications. While the electromagnetic radiation is being applied, the electrons accelerated in linear accelerators turns into electromagnetic radiation through tungsten targets. Electrons and protons as particle radiation are used for head and neck tumors. While electrons are used for superficial tumors, protons are being innovated for deeper tumors even if they are also proper for superficial tumors today.

2.5.1 Conventional two dimensional radiotherapy technique

Before the radiotherapy techniques are improved, the commonly used external radiotherapy technique was conventional radiotherapy, which includes one to four field irradiation by referencing x-ray images of bone structures. In conventional technique lead blocks was produced individually to shape the incident radiation from old cobalt devices. Opposite fields, covering the tumor bed and neck lymph nodes was used.

2.5.2 Three dimensional conformal radiotherapy (3DCRT) technique

As the imaging techniques are improved, modern linear accelerators guided with these imaging techniques are improved. Using multileaf collimator (MLC) systems, tumor volumes are started to irradiated with sharp bounders. As the planning techniques and the devices are improved, three dimensional conformal radiotherapy (3DCRT) became the main external radiotherapy technique. The new technique included CT images and allowed to see and use three dimensional information of the tumor. In 3DCRT technique, three dimensional images of the each organ could be produced and it is possible to calculate how much dose each critical organ absorbed, by using the Planning systems simulating the irradiation fields and the absorption (Khan 2014).

2.5.3 Intensity modulated radiotherapy (IMRT) technique

With the technology being improved, the radiotherapy is also improved. After 3DCRT applications, a new technique including MLC movement and intensity changes of radiation started to be used with better algorithms using optimization codes predicting the best gantry angles and radiation intensities for desired dose distributions. This technique is named as intensity modulated radiotherapy (IMRT) and it recently became the standard type of external irradiation (Khan 2014).

IMRT differs from 3DCRT with sub segments produced by different MLC positions to set the best dose distribution for non-homogenous tumor margins and to lower the doses for critical structures (ICRU Report 83).

The principle of IMRT is combining the ideal gantry angles with proper radiation intensities and proper MLC openness. The planning systems innovated for IMRT arrange the most reliable treatment plans when the priorities and the dose limitations are introduced to the system correctly (Khan 2014).

Producing an IMRT plan can be summarized as follows: Critical structures and tumor volume are contoured according to definitions in International Committee of Radiation Units (ICRU), on images imported from CT device, by physicians, as given Figure 2.2.

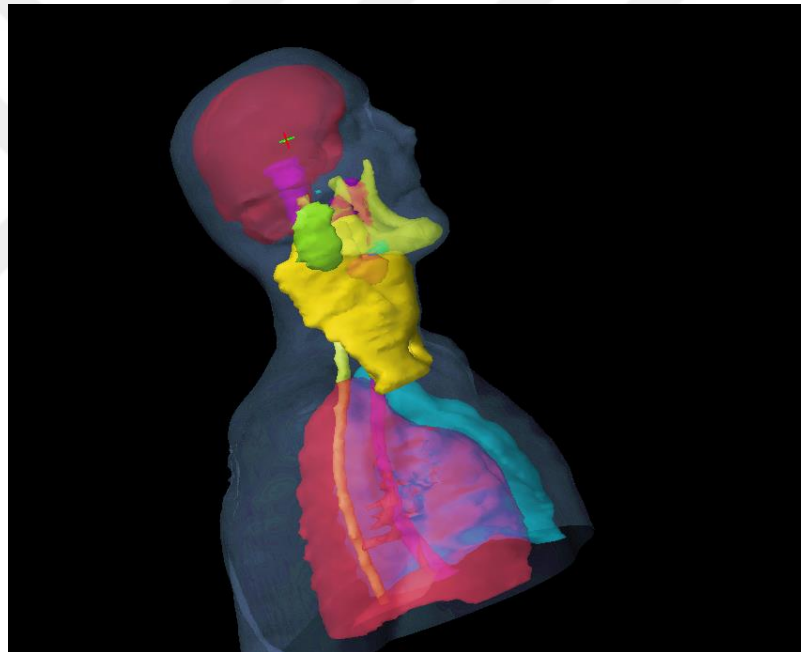


Figure 2.2 Contoured Critical Structures and Target Volumes on CT Images

Gantry angles should be chosen or can be optimized by optimization codes, as given in Figure 2.3. Then the dose constrains and desired doses for each region are defined in the computer. If the inputs are entered correctly, without confusing the algorithm, the planning systems gives the best possible MLC positions for treatment after some iterations. Iterations can continue until the desired constrains are obtained, or they can be started from the beginning if the desired doses are not obtained. After MLC position

obtained by highly precise patient setup with the help of immobilization systems and dosimetry systems (Yeh 2010).

2.6 Skin

2.6.1 Skin layers

Skin consists of three layers called epidermis, dermis and hypodermis. Outer layer, epidermis is about 0.07mm thick. Epithelium cells are located in this layer, which is the most radiosensitive layer. Dermis layer, including many blood and lymphatic vessels, fat and sweat glands and neurons, is located under the epidermis layer. Under the dermis, the innermost layer is hypodermis (Kwan et al. 2008). Due to the over irradiation, at early stages, erythema and desquamation may occur at epidermis. At dermis, late effects like hypoxia, telangiectasia, necrosis or fibrosis may occur (Yu et al. 2003). Increase at acute toxicity is observed at head and neck patients. These increasing skin reactions are thought to be related with thermoplastic masks (Bahl et al. 2012).

2.6.2 Skin doses

Photons loses their energy through their path. They transfers their energy to the material they pass through. The absorbed dose by material results with photon matter interactions. At the energies of megavoltage radiation treatments, the Compton Scattering is the dominant interaction. When the beam enters to the body the incident photons produces electrons scattering forwardly. These forwardly scattering electrons loses their energy at a distance. Until they lose their energy the total, absorbed dose increases. After the absorbed dose reaches at a maximum value, it starts to decrease until it leaves the body. The distance where the absorbed dose reaches at its maximum value is called buildup point. The region between where the radiation enters body and buildup point is named as buildup region. As the photon beam does not lose a high amount of its energy at the entrance of the body, the healthy skin tissue is protected. When the target is skin, a tissue equivalent material called “bolus” is placed directly on the skin. Variation of absorbed dose and kinetic energy released in matter (kerma) with skin depth is given in Figure 2.4.

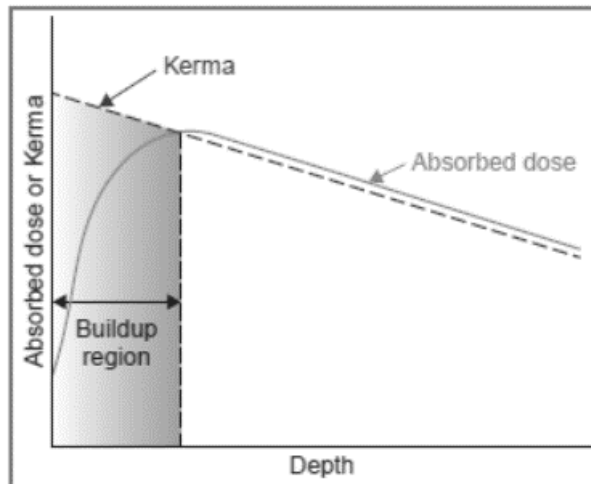


Figure 2.4 Plot of absorbed dose and kinetic energy released in matter (kerma) as a function of depth (Khan 2014)

As the forwardly scattering electrons are produced, some amount of backscattering electrons are also produced. These backscattered electrons contribute to buildup region dose and skin dose.

Another contribution to skin dose occurs by the contamination caused by linac head. Photons used in radiotherapy cause electron contaminations as they hit the collimators and MLC. The secondary electrons scattered from environment directly contribute to skin dose if they reach the body (Jesper and Vestergaard 2000, Haridas et al. 2006, Khan 2014).

2.7 Immobilization Systems for Head and Neck Radiotherapy

Success of the radiation treatment depends directly on the radiation being sent to the right point of the target. Wrong positioning of the patient causes inadequate irradiation of the tumor, while causing more irradiation on healthy tissues. Positioning the patient and organ movements due to the inspiration and expansion can be counted as examples of tumor location changing factors. Effect of inspiration and expansion is being neglected until recent years but positioning the patient correctly is always a fundamental problem for radiotherapy. To decrease the error of the irradiation, the patient should always be positioned as the initial position. Repetitive sessions of radiotherapy necessitate the use of immobilization systems.

Immobilization systems have a vital importance in fields with small margins and full of critical organs such as head and neck region (Perez and Brandy 2013). Head and neck support pillows and thermoplastic masks are two of the most common using immobilization systems for head and neck region.

2.7.1 Head and neck support pillows

Patients' neck is supported with a rigid pillow. The pillow keeps patient's neck in same position on treatment sessions and allow patient stay in comfort during the treatment. There are a few different height support pillows according to concavity of the head and neck. Pillows in different heights are given in Figure 2.5.



Figure 2.5 Head and Neck Support Pillows (http://www.bcc.taipei/RTproducts/product_timokit.html 2018)

2.7.2 Thermoplastic masks

Thermoplastic masks are immobilization materials most commonly used for head and neck treatments. These masks provide accurate positioning and limit the movement of the patient. But, the scattered and backscattered radiation doses due to the mask may cause undesired doses in the skin. However, in most studies it is shown that these over skin doses may be ignored when the benefits of the masks are considered. Thermoplastic masks are given in Figure 2.6.

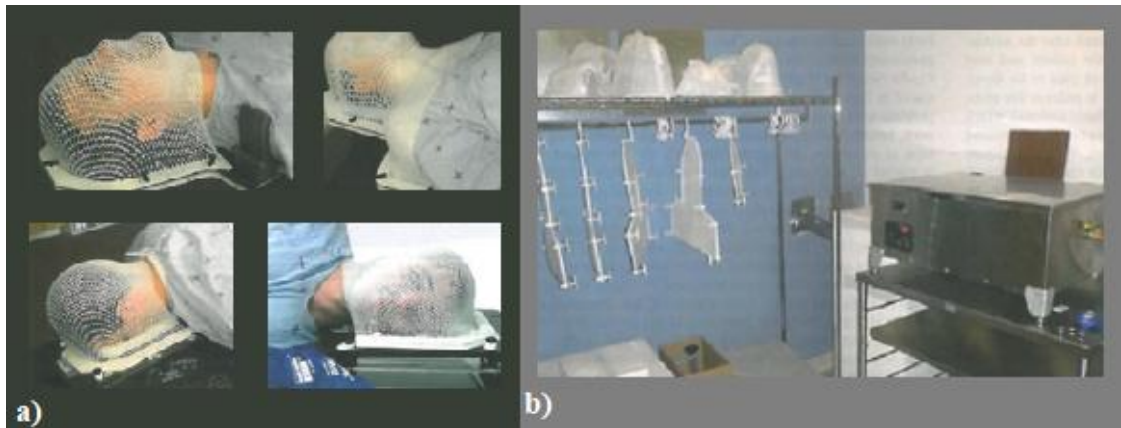


Figure 2.6 Appliated Thermoplastic Masks, Thermoplastic Masks and Heating Bath (Perez and Brady 2013)

Before applying on the patient, the thermoplastic masks are heated in 70°C water baths to become elastic, Figure 2.7. When they are in that elastic form, they are applied to the patient's face and when they cool down, they become rigid and inelastic. These masks are used from the beginning of the treatment until the end of the treatment. If any deformation of elasticity is observed in these masks, the masks can be reshaped for the patient and the treatment plan may be reproduced from the beginning.



Figure 2.7 Thermoplastic Mask Inside a Bath

These masks are immobilized to a secondary couch located on the main treatment couch. Ideal immobilization systems are expected to be in an inflexible rigid form and not to decrease the quality of the treatment beam. While these immobilization systems provide accuracy for the positioning of the patient, these systems may be confusing for the old version of TPS calculations. Thus, the effect of the immobilization systems should be considered and measured if unexpected side effects are observed.

2.8 Quality Assurance in Radiotherapy

The purpose of the radiotherapy is protecting the surrounding healthy tissue while irradiating the tumor volume with the prescribed dose. The necessity of protecting the environmental tissue more and covering the tumor with prescribed dose in sharper margins results in improvements in radiotherapy techniques. After the radiotherapy techniques started to improve and IMRT technique has been commissioned, it is required to set up quality assurance programs and verify the accuracies, tolerances, and specifications of the system. Verifying the accuracies includes mechanical controls and dosimetric calibration and controls of the linacs and verification of the treatment plans (Khan 2014, Ewrierhurhoma et al. 2015). Treatment plan verifications can be done by measuring the surface doses and comparing it with the TPS doses.

According to where the measurement is done, verification measurements are classified in two groups: *in vivo* and *in vitro*. *In vivo*, in Latin, means “within the livings”. Thus, *in vivo* dosimetry in radiotherapy means radiation dose measurements of a patient directly recorded from his body during treatment. Counterwise, the words “*ex vivo*” or “*in vitro*” represents the measurements made before or after the treatment session using a phantom instead of the patient (Mijnheer et al. 2013).

2.8.1 In vitro dosimetry and phantoms

It is not possible to make calibrations and measure all the doses on a patient. In order to calibrate the radiotherapy relevant devices, reference structures called phantoms are produced. Phantoms are structures that make calibration and dosimetric measurements easier in the linacs. Water is used as reference dosimetric material in measurements and calibrations in linacs. However, it is not practical to use liquid water systems all times. Therefore, phantoms are produced in solid form and with chemical properties close to

water or human tissues. There are phantom varieties available on the market for various purposes; such as the Alderson Rando Phantom, the water phantom, the solid water phantom, the virtual water phantoms (Podgorsak 2010).

2.8.2 In vivo dosimetry in external radiotherapy and dosimeters

In vivo dosimetry has been a common and practical way to ensure that the treatments are carried out as they are intended (IAEA Human Health Reports No. 8 2013).

In vivo dosimetry requires a detector to be placed on the patient's body or close to patient anatomy. As the placed detector is irradiated together with patient, it shows the same doses with absorbed dose by the patient, thus it allows to detect major errors and to assess clinical differences between planned and delivered doses (Mijnheer et al. 2013).

In vivo dosimeters can be generally categorized as real-time or active dosimeters and passive dosimeters. Both dosimeters produce radiation induced signals but active dosimeters display a direct number of the detected dose or dose rate in real time while passive dosimeters store the signal and the results are read with the help of various equipment (Canadian Nuclear Safety Commission 2011).

Active in vivo dosimeters cover a group of detectors including EPID, diodes, plastic scintillators and, metal oxide semiconductor field effect transistors (MOSFET). They allow to measure the doses during radiotherapy sessions (Mijnheer et al. 2013). In the following some examples to active dosimeters were given with their advantages and disadvantages:

Diodes as an example to active dosimeters, allows instantaneous readout of measured dose. They are produced small and they have commonly been used as in vivo dosimeters. Their reliability and high sensitivity make them preferable in many clinics but their cables connecting the detectors placed on the patients, to the electrometer placed on the outside of the treatment room makes these detectors impractical (IAEA Human Health Reports No. 8 2013, Mijnheer et al. 2013).

Metal Oxide Silicon Field Effect Transistors or MOSFET are produced significantly small. They can easily be placed in the body cavities which makes them advantageous especially in brachytherapy applications. Although they do not need cables connecting

them to outside of the room, they have complex and sensitive cable connections in the treatment room. Their limited lifetime and complex, sensitive cables slowing the setup process may be counted as their disadvantages (IAEA Human Health Reports No. 8 2013).

Electronic Portal Imaging Devices or EPID are flat panel detectors made of amorphous silicon. They have been innovated for obtaining portal images during treatment in digital format, mainly to prevent setup errors. Besides this, EPID provide two-dimensional or three-dimensional dosimetric information of the actual dose delivered to a patient. This feature is a useful dose verification method for complex plans like IMRT and VMAT. Their over – sensitivity to low energy photons may be counted as their disadvantage (Mijnheer et al. 2013). Some examples to active dosimeters are given in Figure 2.8.

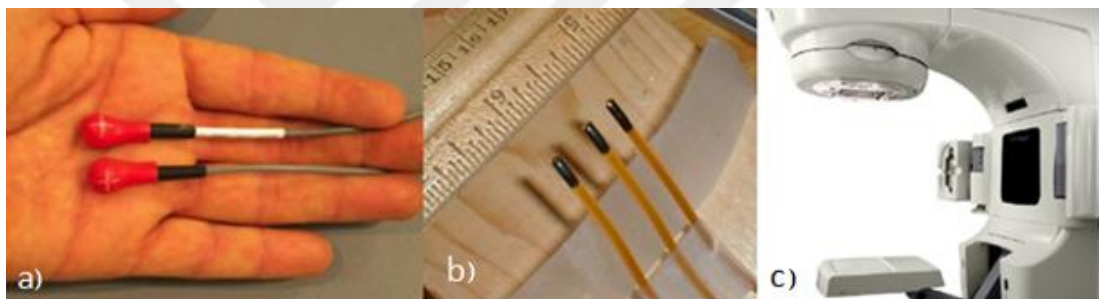


Figure 2.8 a) Diode Dosimeters (http://www.myradiotherapy.com/general/treatment/Treatment_Machines/diodes/Diodes.html 2018), b) MOSFET Dosimeters (http://www.rpi.edu/dept/radsafe/public_html/instruments.html2018), c) EPID on a Linac Gantry (<http://www.medicalexpo.com/prod/varianoncology/product-70440-424098.html> 2018)

Passive dosimeters cover a group of dosimeters including TLD, optically stimulated dosimeters (OSL), film- radiographic dosimeters, radiochromic film dosimeters, gel dosimeters. When exposed to radiation, they record the amount of the radiation exposed. Afterwards, these records are read with help of some electronical systems or without electronical systems if the amount of the radiation is not important. Passive dosimeters allow to measure radiation exposure during a period. In radiation facilities the employees carry passive dosimeters as personal dosimeter. There are some passive dosimeter examples in Figure 2.9.

Radiochromic films are passive dosimeters and radiographic films that do not require long reading procedures like traditional old radiographic films. As the film is irradiated, it changes color. With the accuracy using smaller than millimeters spatial resolution, these dosimeters provide two dimensional dose verifications (Babic and Jordan 2012).

Gel dosimeters are one of the popular dosimeters in medical physics. They are made of radiation sensitive polymers. They are placed in transparent tubes. As these dosimeters are irradiated, chemicals of dosimeter are polymerized due to the absorbed dose. This mechanism allows observing the three dimensional dose distribution and this creates significant advantages on verification for IMRT, stereotactic radiosurgery and brachytherapy applications (Baldock et al 2010). But their complex and toxic production and calibration process, and short lifetime may be disadvantage for clinical usage.

TLD – OSL Dosimeters are one of the most commonly used passive dosimeters in medical applications. Absorption of radiation may retain part of the absorbed energy in trapped states in some materials. Because of the thermal or optical stimulation, when this energy is subsequently released in the form of visible light, this phenomenon is called luminescence. If the stimulator is light, the dosimeters are named OSL, if the stimulator is heat, the dosimeters are named TLD. Although the luminescence dosimetry is practical in clinical use, it requires expensive and complex reading systems (Podgorsak 2010).

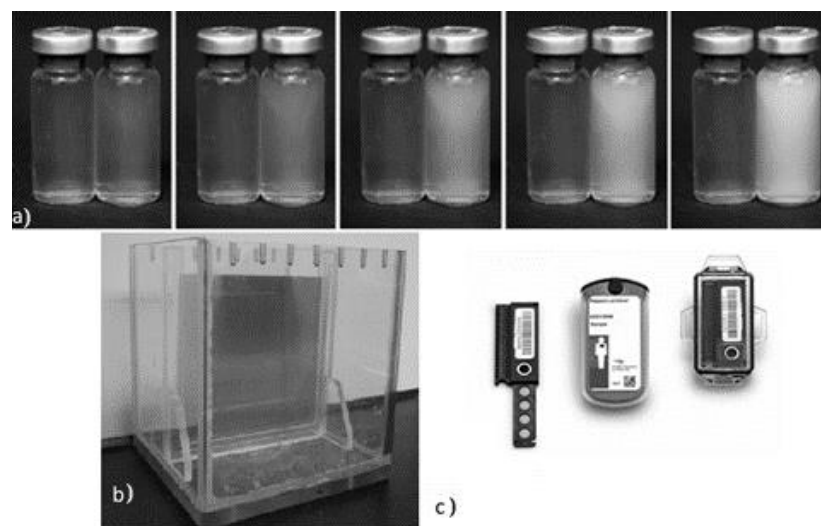


Figure 2.9 a) Gel Dosimeters Irradiated with Different Doses (Gear et al. 2011), b) Radiochromic Film Located in a Plexiglass Apparatus (Babic and Jordan 2012), c) OSL Dosimeter for Individual Use (<https://www.nagase-landauer.co.jp/english/inlight/technology.html> 2018).

Active or passive, all dosimeters have their advantages or disadvantages of their own. In practice, the most suitable one for the purpose can be chosen when their properties like radiation energy and direction dependence, radiation type, ability to be re-read, dose limits, ruggedness and resistance to water, etc. are considered. Because of ease of setup for masks and for their suitable dose, ranges and sensitivity, TLD are used as dosimetry equipment in this study. More information about thermoluminescence dosimetry is given in the section 2.9.

2.9 Thermoluminescence Dosimetry

Thermoluminescence dosimetry has wide application area starting from archaeological dating to medical radiation dosimetry (Podgorsak 2010). Luminescence means emitting light and luminescence dosimetry is based on the detection of the light emitted from an insulator or a semiconductor, commonly called phosphors, produced as the result of radiation absorption of the insulator or semiconductor material. Thermoluminescence is a method of luminescence dosimetry where the material is stimulated thermally. As irradiated material is heated, it emits visible light proportional with the absorbed radiation dose. There are three main conditions that should be satisfied for thermoluminescence to occur.

- The material should be a semiconductor or insulator.
- The material should store the energy as it is irradiated.
- The luminescence emission should occur as the material is heated (Aboud et al. 2012).

2.9.1 Luminescence mechanism

Luminescence mechanism can be explained with a band theory of solids. This theory includes a valence band (VB), where electrons has the most probability to reside in, a conduction band (CB), where electrons has the second most probability to reside in, and a forbidden region between the other two bands. In an ideal semiconductor or in an ideal insulator, electrons are allowed to stay in valence and conduction bands. They can move from one band to another. But are not allowed to reside in forbidden region. When an electron residing in VB is exposed to radiation, it gets excited and goes to CB. However, there are impurities within the crystal lattice; there is a possibility for electrons to possess

energies, which are forbidden in the crystal. In such cases, instead of going to CB, the electron is trapped in forbidden region. This trapped electron escapes through time or by a stimulator (thermal or optical) and goes back to its ground level (VB). As the result of this escape, visible light is emitted from the material (Bos 2007).

If the electron is not trapped and directly goes to CB and goes back to its ground state this event occurs in a time shorter than 10^{-8} seconds (s) and is called as fluorescence or radioluminescence. Else, if the light release happens in a longer time than 10^{-8} s, it is called phosphorescence (Furetta 2003).

Two luminescence mechanism, fluorescence and phosphorescence, are schematically, given in the Figure 2.10.

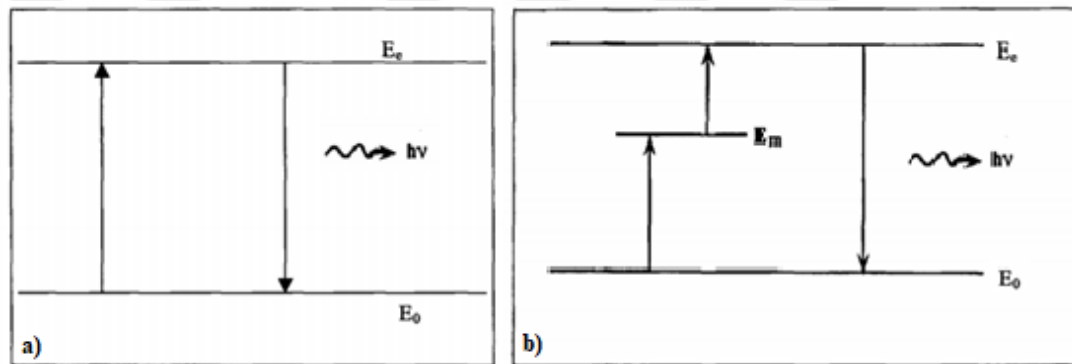


Figure 2.10 a) Fluorescence Mechanism, b) Phosphorescence Mechanism (Furetta 2003)

2.9.2 Thermoluminescence measurement

Even though a small amount of thermoluminescence material is enough for irradiation and depositing energy due to the radiation, TLD require a large system for measuring the results. A simple schematic diagram, Figure 2.11, would help to explain how TLD dosimeter results are obtained.

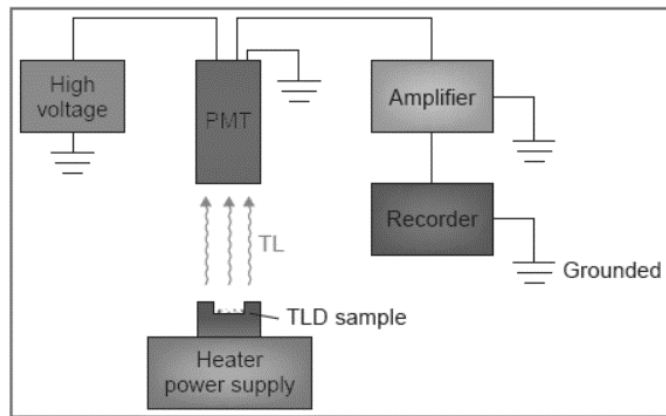


Figure 2.11 Schematic Diagram of a TLD Reader (Khan 2014)

As seen in Figure 2.11, following a preheat process to erase the residual signal, radiation exposed TLD are placed in a cell to be heated through heater power supply. As the TLD are being heated, the probability of trapped electrons to escape from their traps increases and TLD emits light. The light emitted from TLD are detected by a photomultiplier tube and amplified by an amplifier. This system is completed with a recording instrument.

The result is given in a plot of the intensity of thermoluminescence intensity vs temperature and it is called “glow curve”. Glow curve includes peaks. These peaks represents the traps electrons escaped. A lithium fluoride (LiF) glow curve is given in the Figure 2.12. Different peaks show different energy level traps (Khan 2014).

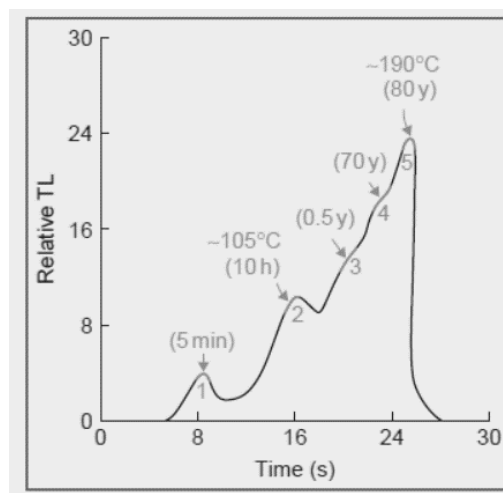


Figure 2.12 Glow-Curve of LiF (Khan 2014)

LiF dosimeters has an effective number of 8.2, which is very close to the soft tissue being 7.4 (Khan 2014). This makes LiF dosimeters to be preferred for clinical dosimetry. LiF chips are also preferred for their small sizes, avoiding the dose changes due to dosimeter. Besides them, TLD chips provide point dose measurement (Mijnheer et al. 2013). TLD chips may be placed on the skin directly for in vivo surface dose measurements. These measurements are useful for checking the skin doses for undesired skin reactions (Khan 2014).

2.10 Studies Related to the Skin Dose Estimations and Use of Thermoplastic Masks

The aim of radiotherapy is to deliver the desired radiation dose to the target volume. However, radiation affects all the tissues it passes on its way through the target volume. Skin is also affected by this incoming radiation. As shown in Section 2.6.2 and Figure 2.4, the absorbed dose by water is minimum at the entrance depth and increases until the buildup point. This behavior is similar at the soft tissue. The low entry doses protect the skin and this behavior is called as the “skin sparing effect”. However, when the auxiliary structures, such as bolus or thermoplastic masks, are used on the skin for radiotherapy, the incoming beam starts to interact with these structures and radiation begins to be absorbed in these structures. Due to these structures, the absorbed dose rapidly increases and it may vary depending on the structure and thickness of the auxiliary material used (Mellenberg 1995).

Even though the skin sparing effect exists, side effects due to radiotherapy are expected in head and neck patients. This is seen in the calculation results of the treatment plans. However, it is generally observed that there are more side effects than expected. These side effects are thought to be mostly due to thermoplastic masks used for patient immobilization. In addition, TPS are inadequate in calculating the input doses, and the thermoplastic mask is not properly added to the skin dose estimations. These factors lead to error in predicting the skin doses.

There are many studies in the literature, either directly measuring the effects of the thermoplastic masks or comparing the measurement results with the planning system calculations. For example, Fiorino et al. (1992) examined the effect of the mask. They measured the doses under the mask and in the absence of the mask using Markus brand

ion chamber. They used 2 and 3.2 mm thermoplastic masks in their study. The masks were irradiated with 6MV x-ray with various field openings, and various source to skin distances (SSD). It is shown that 2mm masks increased the surface doses upto 45% (Fiorino et al. 1992). In another study of Fiorino et al. (1994), the effects of three different brands of thermoplastic masks were compared. In their study, it is shown that different brand masks can change the skin doses in different amounts even if they have the same thickness. In their study, they showed that masks belonging to different brands can increase surface doses from 30% to 62%. Moreover, they showed that the surface dose increased and the skin sparing effect decreased with increased thickness of the masks (Fiorino et al.1994).

A similar study was done by Lee et al. (2002). They applied thermoplastic mask on a rando phantom and irradiated it with IMRT. They measured the doses at the phantom surface with and without mask and they found that thermoplastic masks increased the surface doses by 18% (Lee et al. 2002).

In another study, it was shown by Hadley et al. (2005) that the mask pattern and perforation frequency increased the dose. Depending on the perforation frequency and thickness, the masks increased the surface doses up to 61% when holes were neglected. When 6MV x-ray was applied, small-hole masks increased doses up to 61%, while large-hole masks increased doses up to 52% (Hadley et al. 2005).

More recently, a similar study by Soleymanifard et al. was published in 2014. They applied two different brands of thermoplastic masks to rando phantom. There was no statistically significant difference between the results of the two types of masks. They found that there was no increase in the average surface dose when 15 MV beam was used, but when the 6 MV beam was used they found that the surface doses increased by 20%. According to the results of the vertical and tangential irradiation of the mask, the masks increased the surface dose by 38% and 22%, respectively when the mask holes were ignored (Soleymanifard et al. 2014).

Another study was published in 2016 by Poltorak et al. They measured percentage depth doses using parallel plate detector and solid water phantoms in the presence and absence of the mask. According to their results, the thermoplastic masks increased the skin doses between 10% and 42% (Poltorak et al. 2016).

From a different point of view, unpredicted side effects observed on the skin can be resulted from unpredicted skin doses. In another words, if the calculations of TPS accounting both the skin doses and thermoplastic masks would be accurate, the side effects would be predicted correctly. There are a few studies in literature comparing the TPS calculations and measurement results for surface doses. Court et al. (2007) observed the uncertainties in surface doses using Eclipse TPS. A phantom was irradiated with IMRT and surface doses were measured with MOSFET detectors. The difference between measurements and calculations was less than 10% in 75% of the results and less than 20% in 94% (Court et al. 2007). A similar study was performed by Zhuang and Olch (2014). They irradiated a pelvic phantom with IMRT plans created with Eclipse TPS. They measured the surface doses with OSL and diode dosimeters and compared the results with TPS calculations. According to OSL comparisons, they found differences up to 2.2%. However according to diode comparisons they found differences up to 10.1% (Zhuang and Olch 2014).

In the above mentioned studies, using Eclipse planning system, the calculated surface doses were compared with in vitro measurements. But, the thermoplastic masks were not used in these studies. These studies showed the uncertainty in the Eclipse TPS's surface dose calculations.

Different planning systems and different dose calculation methods and algorithms are used for different devices in the market. For example, a study using a different accelerator, called tomotherapy, and a different TPS, innovated for that accelerator and named as Corvus, were performed by Qi et al. (2008). Qi et al. measured in vivo skin doses under mask with MOSFET detectors during irradiation of the patients. They compared the measurement results with the calculated skin doses. They observed that the calculated doses were higher than the measured results up to 9.2% (Qi et al. 2008).

A similar study using the tomotherapy device and the Tomoplan TPS was performed by Kinhikar et al. (2009). They measured skin doses in head and neck patients under mask, using TLD and MOSFET detectors. They compared the TPS skin doses with the measured doses. The calculated doses are 8-14% higher than in vivo measured doses (Kinhikar et al. 2009).

In contrast to the algorithm used in Eclipse software, it can be said that the algorithms used in the software produced for Tomotherapy devices somehow add doses accounting the masks to their algorithms but still do not reach a concordant conclusion with full accuracy.

In parallel with literature, head and neck patients who used masks were found to have more skin reactions than expected at the Ankara University Radiation Oncology Department. It is thought that this condition is mask-induced and the effect of the mask is not included in the calculations by TPS. Therefore, in our study, the skin doses were measured under the mask during the irradiation of the patients and the values calculated by the planning system were compared by the doses measured by TLD. The difference was evaluated as the effect of the masks on the skin dose.

3. MATERIAL AND METHOD

In this study, the effect of thermoplastic mask on the skin dose was investigated in patients with head and neck cancer treated with radiotherapy in Ankara University Medical Faculty Radiation Oncology Clinic. This effect was evaluated by comparing the dose values obtained from the calculation results in the radiotherapy planning system with the dose values obtained from the in vivo measurements.

All values were obtained from determined four points for each patient. In order to obtain the dose values at four determined points, patients were first laid on CT couch to receive CT images prior to treatment. After proper positioning, the heated thermoplastic mask was applied to the patient. After the mask was cooled, CT markers were placed on the mask and CT images of the patient were recorded. Then the CT images of the patient were transferred to the computers for planning. During planning, critical structures and target volumes were contoured by radiation oncology specialists. The treatment plans were then created by physicists. Through the plans prepared, the skin doses at the four determined points were read and recorded via TPS. The plans were transferred to the linear accelerator and after the quality control, the plan and the patient were ready for treatment.

In vivo measurements were obtained by inserting TLD into the previously determined points, irradiating those TLD with the patient during the treatment session and reading the TLD afterwards. For this, before the TLD to be used in in vivo measurements, the environmental radiation accumulated on the dosimeters was zeroed by annealing them in the furnaces at the Institute of Nuclear Sciences, Ankara University. Afterwards, they were irradiated in Ankara University Medical Faculty Radiation Oncology Department. After a pre-heating process, the dosimeters were read with the TLD reader in the Institute of Nuclear Sciences and the values required for calibration were calculated. The TLD, which were annealed after the calibrations, were ready to be used again.

3.1 Material

3.1.1 Patients

The study was performed in ten head and neck cancer patient; namely five larynx, four nasopharynx and a cervical esophagus cancer patient. Skin doses of patients were measured in vivo. Information of patients is given in Table 3.1.

Table 3.1 Patient Information

Patient #	Age	Sex	Diagnosis
1	20	Female	Nasopharynx Cancer
2	69	Male	Larynx Cancer
3	59	Male	Larynx Cancer
4	61	Male	Esophagus Cancer
5	85	Female	Larynx Cancer
6	80	Male	Nasopharynx Cancer
7	58	Male	Larynx Cancer
8	53	Male	Nasopharynx Cancer
9	56	Male	Nasopharynx Cancer
10	63	Male	Larynx Cancer

3.1.2 GE Optima 580 RT computerized tomography device

In the study, the GE Optima CT580RT computed tomography device in the Radiation Oncology Clinic of the Ankara University School of Medicine, given in Figure 3.1, was used to obtain the tomography images of the patients. The device has a gantry with an opening of 80 cm and a viewing area of 65 cm. The scan unit receives 18 cross-sectional images at a full rotation of the gantry. The thickness of the cross-sectional images can be adjusted from 1 mm to 10 mm.



Figure 3.1 GE Optima 580 RT Computed Tomography Device, Ankara University Department of Radiation Oncology

3.1.3 Thermoplastic mask

Thermoplastic masks are one of the most widely used immobilization and positioning devices. Before applying to the patients, the masks are flat and hard. These masks are softened in a 70°C water bath to become flexible and formable. After applying the masks on the patients, these masks solidify while cooling down. Masks are for individual use only. Same mask is applied on the patient during the treatments. It is very important that the masks do not stretch or lose their shape after repeated use. In this study, IMRT masks (IMRT Mask, RADON) available in the Ankara University Faculty of Medicine Department of Radiation Oncology, were used for measurements. Figure 3.2 shows different stages of a thermoplastic mask preparation. Figure 3.2 (a) shows solid and unshaped thermoplastic IMRT mask , prior to use, Figure 3.2 (b) shows the heated mask in shapeable form, and Figure 3.2 (c) shows the mask after being applied to the patient. The mask is shaped on the patient and according to his/her head and shoulder.

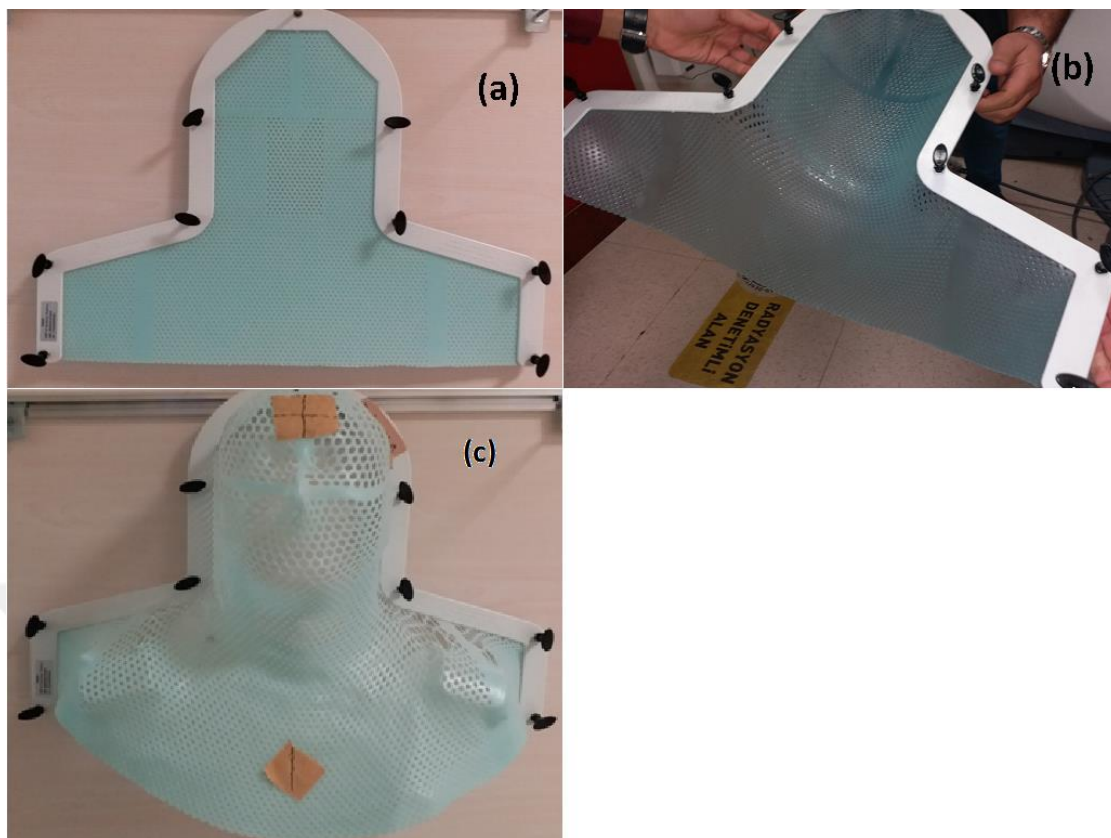


Figure 3.2 Thermoplastic Mask in Ankara University Faculty of Medicine Department of Radiation Oncology and its Appearance at Different Stages of Application a) Unshaped, Rigid b) Heated, Soft, Flexible, c) Shaped, Rigid

3.1.4 CT marker

In this thesis, CT markers (Visionmark model, Suremark) in Ankara University Faculty of Medicine Department of Radiation Oncology were used to introduce the position of the patient to the planning computers and the linac. The sample CT marker is given in Figure 3.3.

CT markers are very small spherical materials made of non-metallic dense material that create a distinct contrast in CT images. These materials are placed on the masks at the projections of the lasers used for patient positioning. They are shown on a single image in transverse section in tomography images and used to introduce a reference point to planning computers. The points where these CT markers are placed are drawn with a pen on the mask and are matched with lasers when positioning during treatment. This is ensured that the plane created in the virtual plane is matched with the real plane.

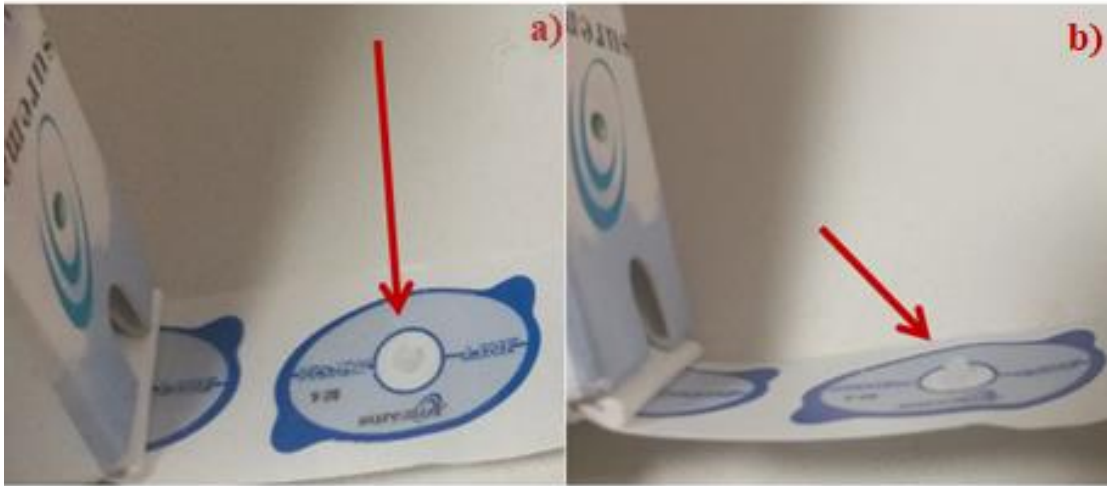


Figure 3.3 Different Views of a Representative CT Marker a) Top View, b) Side View, Ankara University Faculty of Medicine Department of Radiation Oncology

3.1.5 Eclipse TPS

In this thesis, the Eclipse version 10.0.0 TPS in the planning computers of Ankara University Faculty of Medicine Department of Radiation Oncology was used to create the treatment plans of the patients and to record the planning system data. Eclipse is a planning system that prepares data on the Varian Clinac DHX linac device in the clinic. It uses the anti-anisotropic algorithm (AAA) and Pencil Beam Convolution algorithm in its calculations. Images of patients who have previously undergone tomography are transferred to this software. Critical structures and target volumes at the tumor site are contoured by clinicians in the clinic. The total external volume, in other word the body contour, and contours such as the treatment bed, are determined automatically by the software. Guided by these contours, health physicists formulate treatment plans. After approval of the treatment plans, the plans are sent to the linear accelerator with a software called Aria. Figure 3.4 shows an interface from the Eclipse TPS. This interface gives a view from the first steps of radiotherapy planning. It chooses the proper gantry angles for the ideal dose distributions. The interface includes the transverse, the coronary and the sagittal cross sections of CT images and the three-dimensional plane of the patient with the beam.

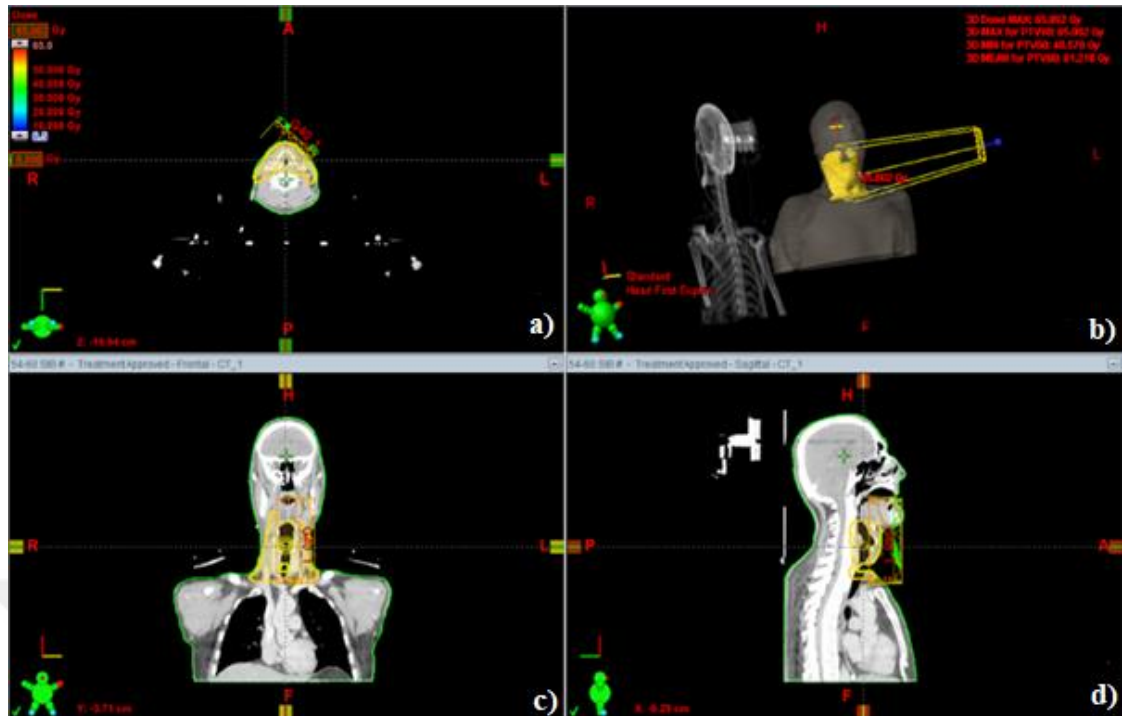


Figure 3.4 Planning Interface of TPS in Ankara University Faculty of Medicine Department of Radiation Oncology, (a) Transverse (Axial) Cross Section, (b) Three Dimensional View of Patient, (c) Coronal Cross Section, (d) Sagittal Cross Section

3.1.6 Varian Clinac DHX linear accelerator

In this thesis, Varian brand Clinac DHX model linear accelerator in the Ankara University Faculty of Medicine Department of Radiation Oncology was used for TLD calibrations and irradiation treatment of the patients. The Varian Clinac DHX linear accelerator given in Figure 3.5 is a treatment device that allows 3DCRT and IMRT applications. It enables the implementation of dynamic IMRT using 120 MLC. 40 MLC located in the middle of the MLC system are 0.5 cm, the others are 1 cm wide. The treatment area can range from 0.5 cm x 0.5 cm to 40 cm x 40 cm. The device enables 6Million electron volt (MeV), 9MeV, 12MeV, 15MeV, 18MeV, 22MeV energy electron treatments with 6 Million Volt (MV) and 18MV energy photon treatments. There is an EPID in front of the gantry system. This device receives images of patients with high-energy x-rays and allows for a more accurate position before treatment.



Figure 3.5 Varian DHX Linear Accelerator, Ankara University Faculty of Medicine Department of Radiation Oncology

3.1.7 TLD chips

In this study, TLD chips in the Radiation Oncology Clinic of Ankara University Medical Faculty were used to measure the radiation doses that the patient skin was exposed to. TLD dosimeters are the most commonly used dosimeters to measure radiation exposure. TLD dosimeters are made of LiF material including Magnesium (Mg) and Tallium (Tl), produced in a wide range of sizes and shapes. TLD dosimeters are considered as tissue equivalent dosimeters due to the effective atomic number of 8.2, which is close to 7.4, which is the effective number of human tissue (Khan, 2014).

In this study, the rectangular prism and cylindrical TLD chips, given in Figure 3.6, are used. The two types of dosimeters are different in shape and mass only. Rectangular prism TLD have dimensions of 3.1 mm x 3.1 mm x 0.9mm and cylindrical dosimeters are 4 mm in diameter and 1 mm in height. This causes different amounts of light to emit when they take the same dose in relation to their difference masses. This difference can be eliminated by correction factors.

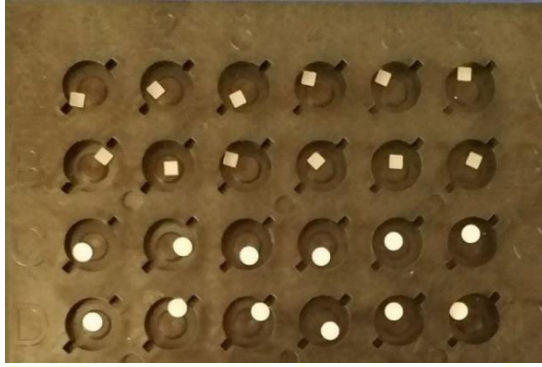


Figure 3.6 TLD Chips, Ankara University Faculty of Medicine Department of Radiation Oncology

3.1.8 Solid water phantoms

In this thesis, solid water phantoms found in Ankara University Faculty of Medicine Department of Radiation Oncology, Figure 3.7, have been used. Solid water phantoms in the Clinique are 40 mm x 40 mm wide having thicknesses of 1 mm, 2 mm, 5 mm and 10 mm. The solid water phantoms were used during the calibration processes of TLD.

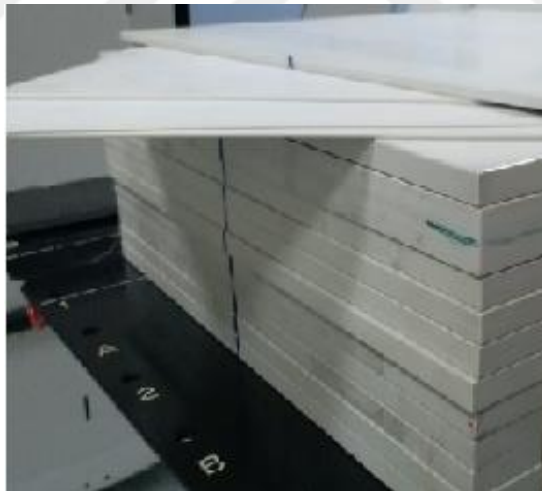


Figure 3.7 Solid Water Phantoms in Different Thicknesses, Ankara University Faculty Of Medicine Department Of Radiation Oncology

3.1.9 PTW -TLDO TLD annealing oven

In this thesis, the PTW-TLDO TLD Annealing Oven at the Ankara University Institute of Nuclear Sciences, Figure 3.8, was used in preheating the irradiated TLD and in

annealing process. There are two heating programs in the oven. The first is a preheating mode that allows to clean signals by draining unstable traps with heating the TLD before reading. The preheat mode takes approximately 30 minutes. In this program, the oven first heats the TLD to 100°C and maintains it at this temperature for 10 minutes. Then it allows the TLD to cool to room temperature. The second program is the annealing program. This program is run after TLD are read. This mode heats the dosimeters up to 400°C and maintains for one hour at that temperature. Then it goes into cooling mode. The device keeps its temperature for two hours when it reaches at 100°C. The oven can heat 360 TLD in its drawers and stainless steel heating plates that can be seen in Figure 3.9 ([https://www .radat.com.tr/dochuments/tld-oven.pdf](https://www.radat.com.tr/documents/tld-oven.pdf) 2018).

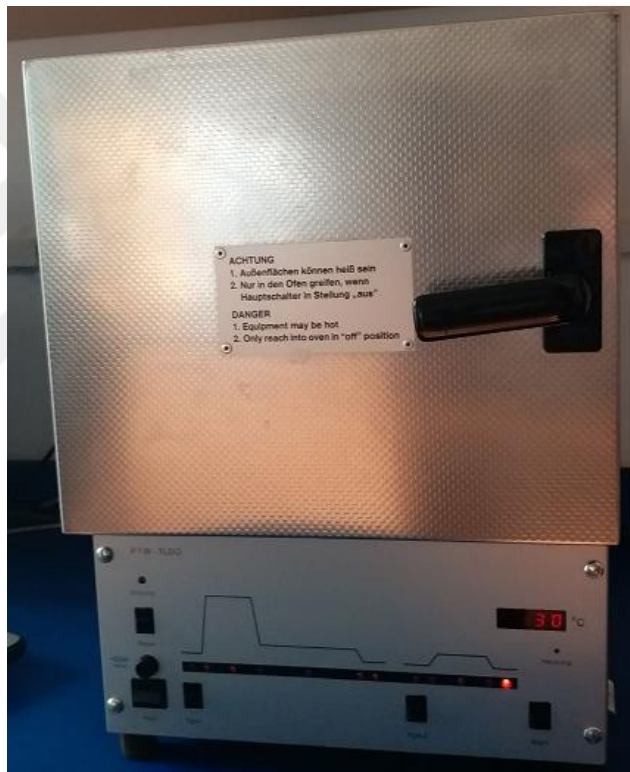


Figure 3.8 PTW- TLDO Annealing Oven, Ankara University Institute of Nuclear Sciences

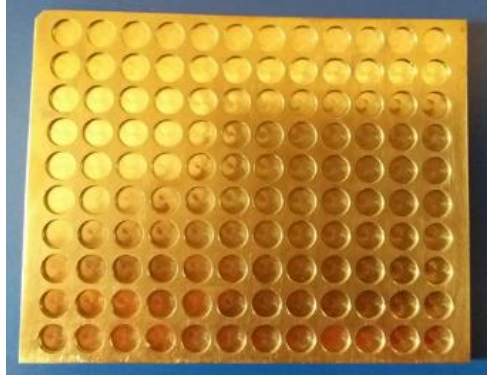


Figure 3.9 Stainless Steel Annealing Tray, Ankara University Institute of Nuclear Sciences

3.1.10 Harshaw TLD model 3500 manual reader

In this study, Harshaw TLD model 3500 manual reader in the Institute of Nuclear Sciences of Ankara University, Figure 3.10, was used to read radiation exposed TLD. The reader has a drawer that allows only one TLD to be read at a time. The TLD placed in this drawer is heated by the reader. TLD emits detectable light as it is heated. This light is amplified by photomultiplier tubes and then converted to electrical charge and current. The magnitude of the generated electrical current is proportional to the radiation dose to which TLD is exposed. A software called WinREMS allows user to see the value of the intensity of light detected by the Harshaw reader in terms of the Coulomb unit (<https://www.thermofisher.com/order/catalog/product/3500TLDDS3> 2018). Before reading, some parameters such as preheat temperature and duration, maximum heating temperature, heating speed are entered into WinREMS program and these parameters are directed by the reader.



Figure 3.10 Harshaw TLD 3500 Manual Reader, Institute of Nuclear Sciences of Ankara University

3.2 Method

3.2.1 Planning system calculations

Calculated doses of patients were recorded from TPS. But firstly the patients were prepared for radiotherapy. After their preparation process, treatment plans were created and the points where the doses would be recorded were determined. The mean absorbed doses were recorded as the calculated dose for each determined point.

3.2.1.1 Preparation of patients for the treatment

Firstly, patients were laid on CT table to receive CT images prior to treatment. Patients receive treatments around twenty-five to forty working days. Considering the duration of the treatments, the patient must be laid in such a position that he/she is both comfortable and not difficult to breath. The patient was also supposed to repeat the same position in each treatment. Therefore, using a radiotherapy cushion to support the patient's head, the patient was able to lie comfortably in the supine position. A scout image was taken before the tomography image to see if there was a difference in the patient's position from the desired position. When the desired position was given to the patient, the heated thermoplastic mask was applied to the patient, Figure 3.11.



Figure 3.11 Preparation of Thermoplastic Mask for Patient

After the mask was shaped and cooled, CT markers were placed on the mask and the patient's tomography images were taken at 2.5 mm section intervals, Figure 3.12.

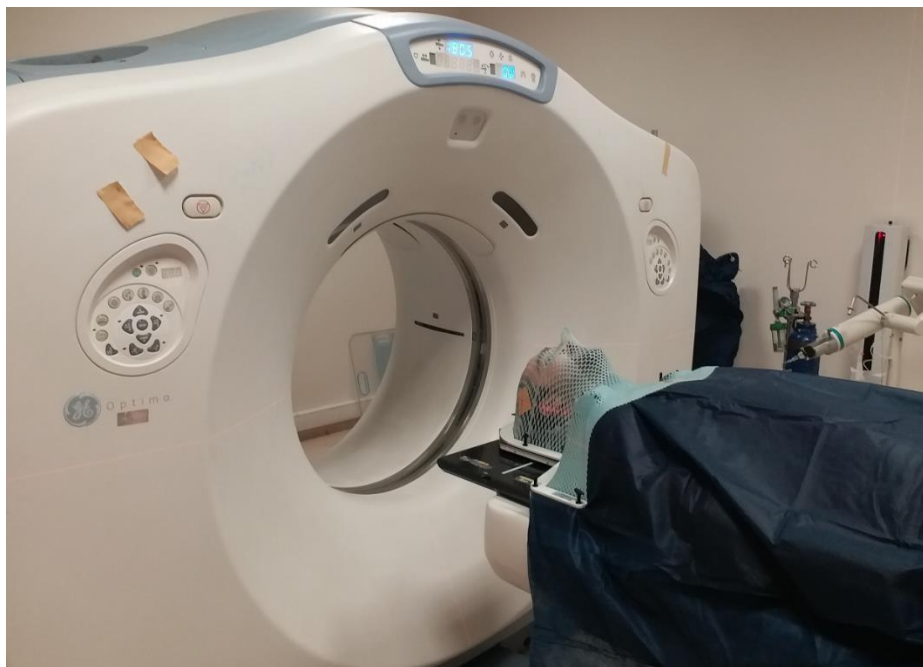


Figure 3.12 Patient's Being Prepared to Take Tomography Images

After the CT images of the patient were taken, these images were transferred to the planning computers. During planning, the critical structures, Figure 3.13(a), and target structures, Figure 3.13(b), were contoured by radiation oncology specialists.

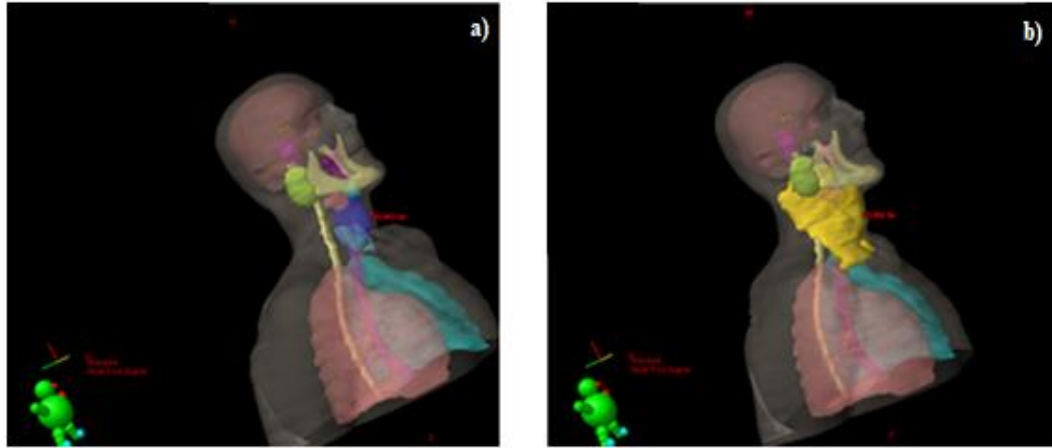


Figure 3.13 a) Critical Structures, b) Target Volume in Yellow and Critical Structures

Afterwards, the treatment plans were created by physicists using IMRT technique. A total of two types of angle groups were used during the preparation of the plans. These angles are either 20° , 60° , 100° , 140° , 180° , 220° , 260° , 260° , 340° in a group or 0° , 40° , 80° , 120° , 160° , 200° , 240° , 280° , 320° in another group.

3.2.1.2 Determination of the points that will be measured from TPS

For each patient for both measurement and calculation, four anterior angles, where the radiation was directed through the mask to the patient, were selected, Figure 3.14.

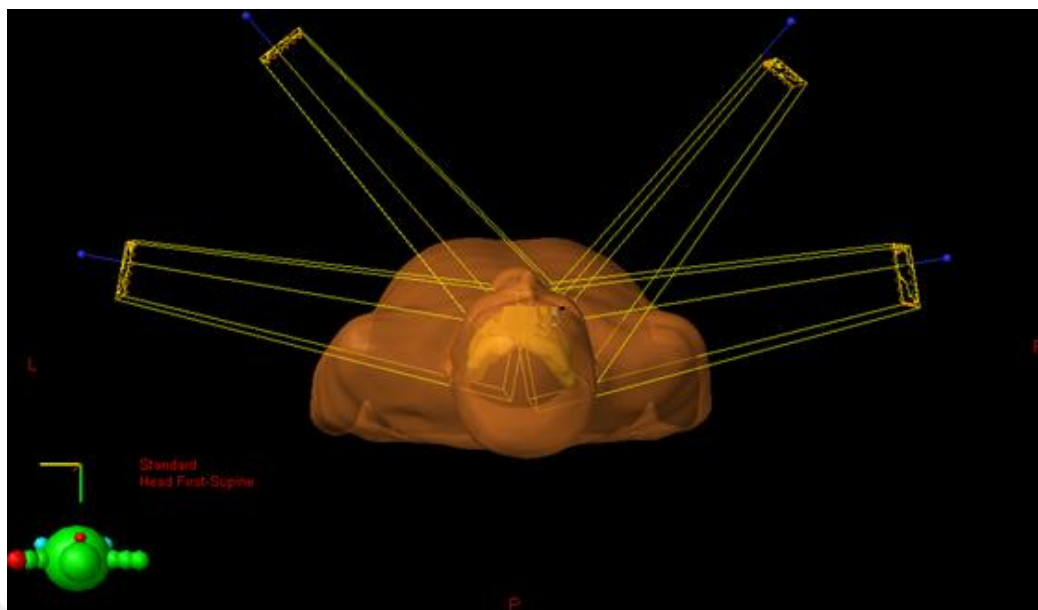


Figure 3.14 Four Anterior Angled Beams were Selected for each Patient

The intersections of 40°, 80°, 280° and 320° were marked in a group of patients, while the remaining patients were marked with intersections of 20°, 60°, 300° and 340°, Figure 3.15.

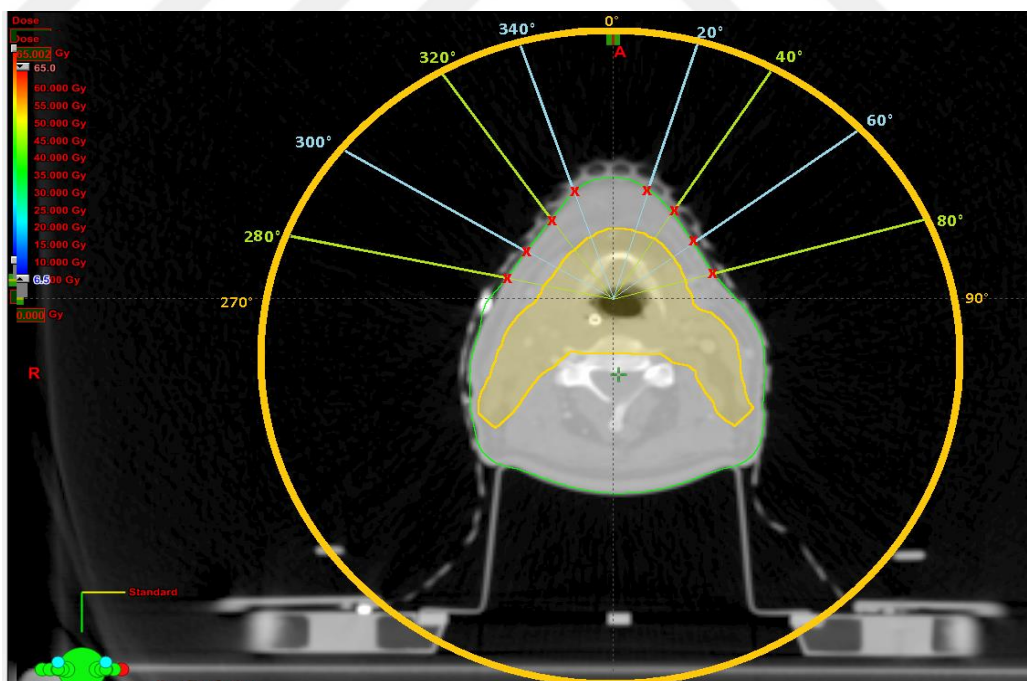


Figure 3.15 A Schematic Diagram Showing Gantry Angles Chosen. Green and Blue Marks Show Different Angle Groups.

The doses calculated by TPS and the doses measured on the patients was compared in the study. It should be noted that it was important that the location of value measured in vivo was exactly the same as the location of value read from the TPS. For this reason, it was necessary to select the points that can be determined both through in vivo and the planning system. In accordance with this situation, in the planning system, intersection of the used beam centers with the skin contour is selected, Figure 3.16.

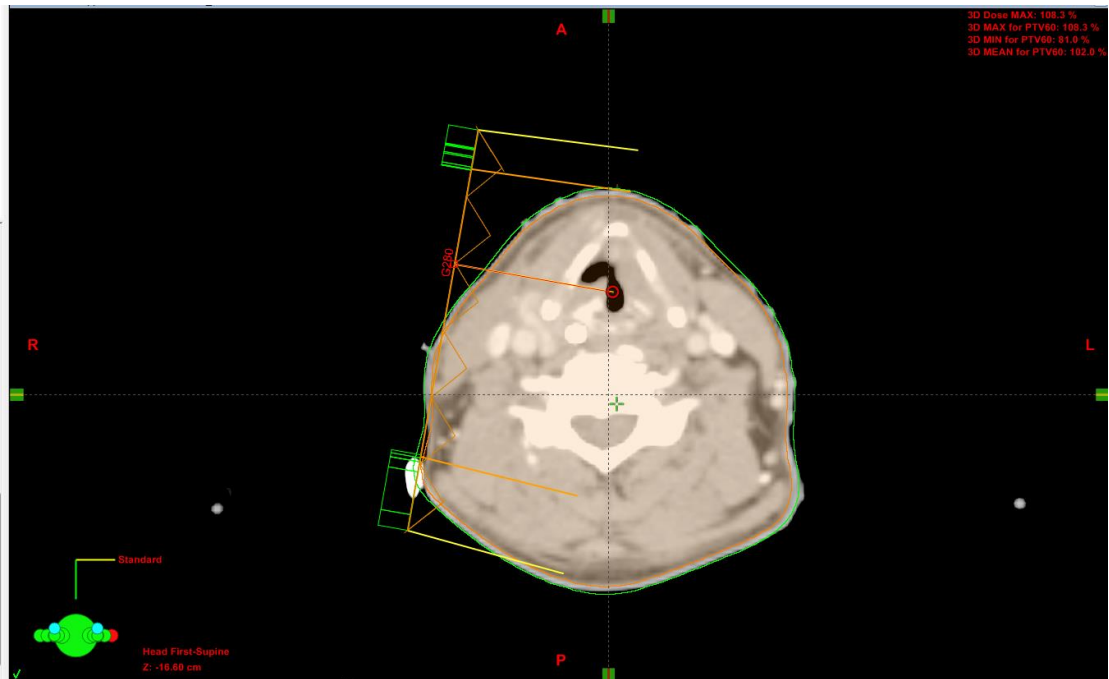


Figure 3.16 Determination of the Calculated Doses at Marked Points

At this point, small volumes representing the TLD were contoured, down from the surface, not exceeding 2mm in depth, Figure 3.17. These volumes are large enough to correspond to the TLD volume. The average dose absorbed by these volumes was recorded as the absorbed dose value of that volume.



Figure 3.17 The Body Contour (In Green), 2 mm Reference Contour (In Orange) and TLD Contours (In Pink) for Calculation

The plans were transferred to the linear accelerator through intra-hospital information transfer network and after the quality control; the plan was ready for the treatment.

3.2.2 In vivo skin dose measurements

Skin doses of patients were measured by TLD placed under the mask in the first days of their treatment. These TLD were irradiated directly with the patient during the treatment and then read subsequently. Before the patients received the treatment, they were laid in the same position with the CT couch at the treatment table. Room lasers were overlapped with the markers on the mask and accuracy was fully obtained by taking the EPID image position. After making sure of the accuracy of the position, patients were irradiated by using their treatment plans. Figure 3.18 shows the location of the patient on the treatment table and the position of the gantry relative to the patient.



Figure 3.18 Patient Positioning and Gantry Rotation

3.2.2.1 TLD preparation for usage

TLD dosimeters must be calibrated before use for accurate measurements. Dosimeters should be exposed to the known radiation doses and then the Element Correction Coefficient (ECC) and Reader Calibration Factor (RCF) for calibration should be calculated. ECC can be defined as a coefficient related with the response of each TLD. When TLD produced with same material, in the same shape and mass are exposed to equal radiation dose, it is expected to emit the same amount of thermoluminescence light, but impurities in the material forming the dosimeters do not actually make this case possible. The differences in the results of TLD can be indicated by the coefficient given as ECC. RCF is a coefficient used to convert the electrical charge value recorded by the reader to the absorbed dose unit while reading the dosimeters.

The irradiations required for the TLD calibration were performed at the Ankara University Faculty of Medicine Radiation Oncology Clinic, and the dosimeters were read at the Ankara University Institute of Nuclear Sciences Individual Dosimetry Laboratory. Before all processes, the TLD were heated in the PTW TLDO oven in annealing mode. Thus, all traps of the TLD were discharged. TLD dosimeters were covered with very thin

plastic foil in order to protect them from environmental factors such as tape and dust. Afterwards, dosimeters were taken to Ankara University Medical Faculty Radiation Oncology Clinic for irradiation. Here, the solid water phantoms were placed on the treatment table of the Varian DHX linac. TLD covered with thin plastic foils were placed in a solid water phantom at a depth of 1.6 cm, in an area of 10cm x 10cm. They were placed separately in order to prevent scattering from each other. The measurement at this depth and field openness at the distance of 100 cm source to skin distance (SSD) is called reference measurement. So with these parameters, the tissue irradiated with 6 MV, 100 monitor unit at a depth of 1.6 cm is expected to absorb the dose of 100 cGy radiation. The preparation of TLD for exposure to the known dose is shown in Figure 3.19. Figure 3.19 a) shows TLD packaged and separately positioned to prevent them from being affected from each other during irradiation. Figure 3.19 b) shows 1.6 cm solid water phantom placed on the TLD and TLD ready for reference irradiation.

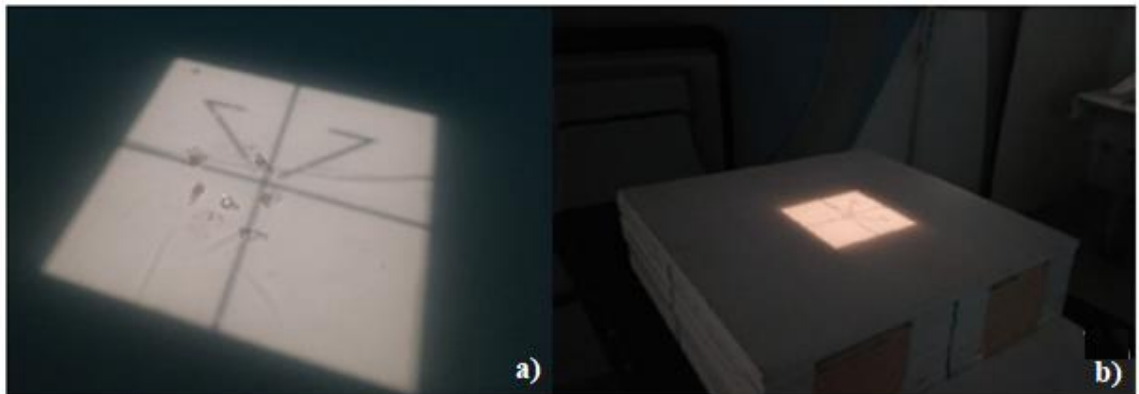


Figure 3.19 Setup for TLD Calibration Irradiation. A) TLD Positioning, B) Placing the Solid Water Phantoms on TLD.

The irradiated dosimeters were placed in the stainless steel plate and furnace at the Ankara University Institute of Nuclear Sciences Individual Dosimetry Laboratory for preheating and the oven was operated in preheating mode. In this mode, the TLD were heated to 100°C, maintained at this temperature for 10 minutes, and then cooled to room temperature under the flow of air in the medium. When TLD reach to room temperature, they were read one by one, by placing them in the Harshaw reader. The parameters of the WinREMS software that guide the Harshaw reader were settled as: preheating

temperature 100°C, maximum temperature 300°C, heating rate 10 °C / s, and waiting time at preheating 10 s.

In the Harshaw reader, each TLD was heated to 100°C and then to 300 °C. Depending on the heating, the thermoluminescence light was emitted from the dosimeters. The emitted thermoluminescence light was detected by PMT tubes in Harshaw. The luminescence detected by PMT tubes was converted to electric current and the current data was transferred to the WinREMS program. These current data represent the radiation doses to which TLD was exposed. The resultant TLD was again cooled to room temperature and taken back from the Harshaw and placed again on the stainless steel plate to be annealed. After all the dosimeters were measured and the current values were recorded, the dosimeters placed in the stainless steel plate were annealed in the PTW TLDO oven.

During the calibration, this process was repeated for all TLD. Then the values obtained from the TLD were recorded on the computer and the standard deviations were calculated. However, in this study, TLD with a deviation of above 5% were discarded from the measurement and rest of the dosimeters were assumed to be identical to each other. The ECC factor was taken as 1 in this case. In addition to this assumption, the RCF factor was calculated by taking the average current values recorded by WinREMS to the radiation exposure used for TLD calibration .

3.2.2.2 Determination of points to be measured

After all the preparations and quality controls the patient received his or her first radiation treatment. At the end of the first treatment session, while the patient was still lying on the treatment couch in treatment position, the linac gantry was turned to the positions marked in the treatment plan. The projections of treatment field centers were marked on the mask as the in vivo equivalents of the regions where the TLD contours were established in the planning system, when the patient was in the treatment position. For each patient, the gantry was placed in four different positions and the projection of the treatment field centers on the patient was marked as shown in Figure 3.20.

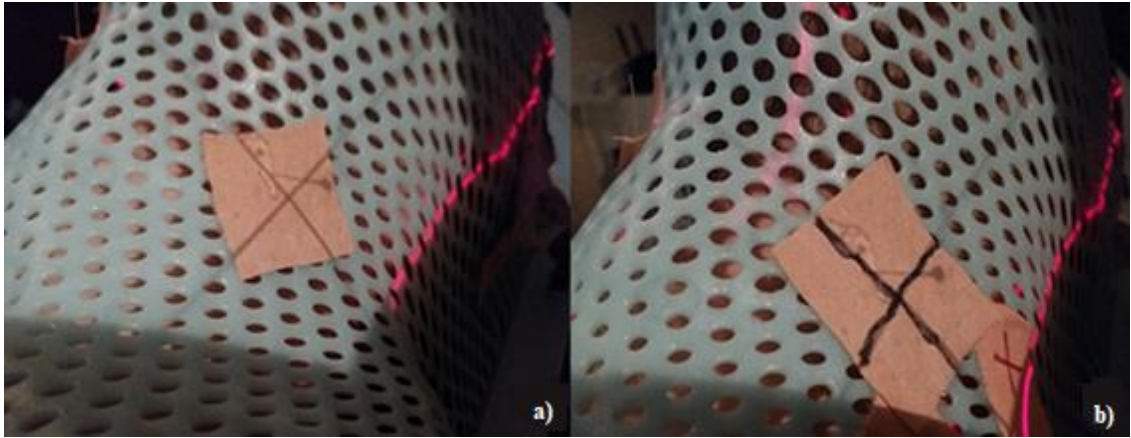


Figure 3.20 Marking the Masks for TLD Location a) Projection of the Treatment Field Center b) Marked Treatment Field Center

The masks marked on the outer surface, were taken out of the radiotherapy room after it was removed from the patient. Afterwards, TLD were placed on the inner surface of the masks at the marked points and they were ready for measurement, Figure 3.21.

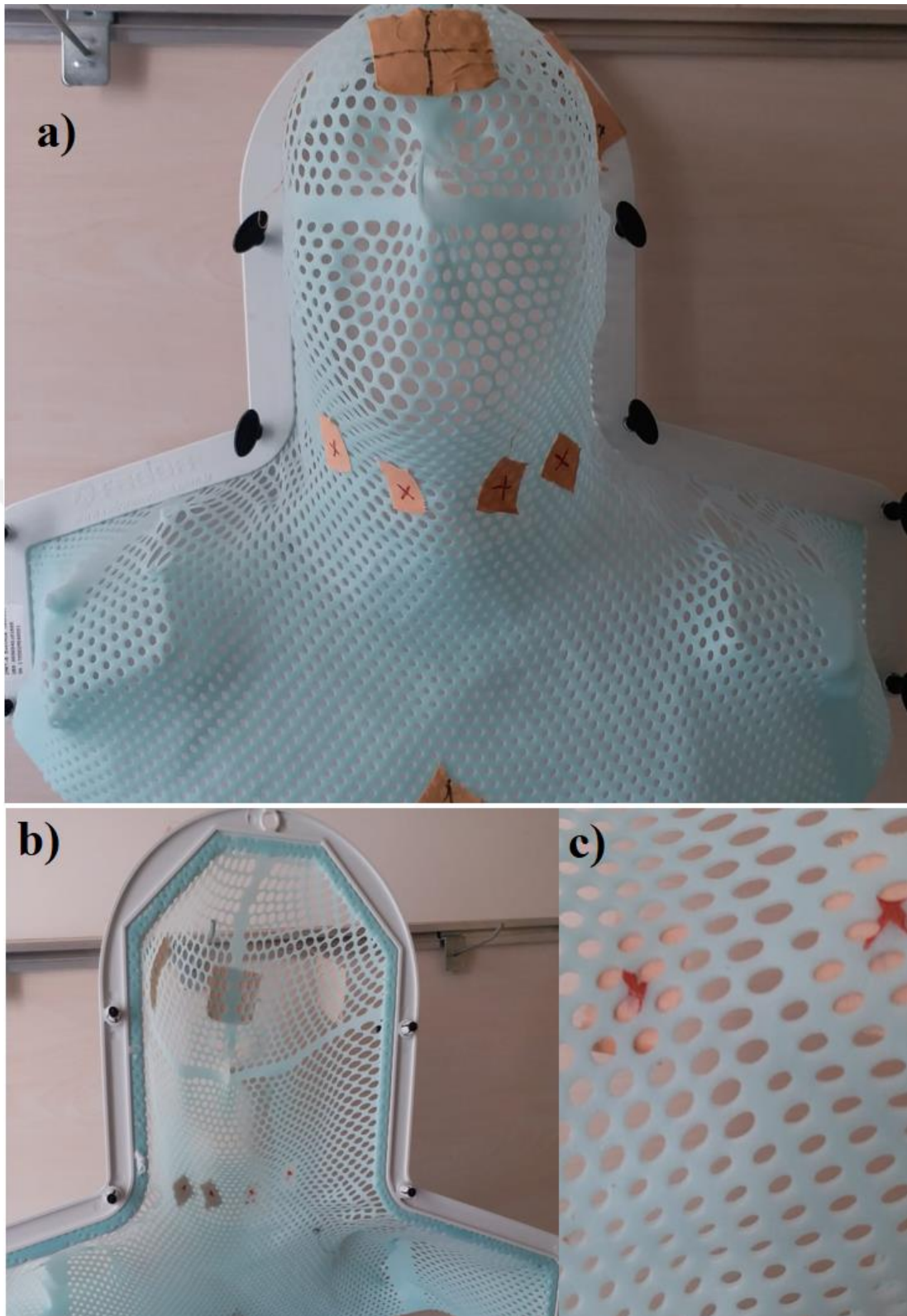


Figure 3.21 Thermoplastic Mask Marked on the Guide of Gantry Angles for TLD Locations a) The Mask Marked During Gantry Rotation b) The Mask Marked on the Inner Surface by the Guide of Outer Surface Marks c) Magnified Inner Surface of the Mask

The masks with TLD were stored away from radiation fields until the patient's next treatment. On the next day, the patient was put on the mask and he/she took the daily treatment. Placed TLD were exposed to exactly the same amount of radiation with skin as they were stuck between skin and mask. At the end of the treatment, TLD were removed from the mask to be read. Different TLD were placed inside the masks for the next treatment and kept away from the radiation field. In this way, the irradiation of TLD on the patient was repeated for three consecutive days for each patient. At the end of these three irradiations, TLD were read at the Ankara University Institute of Nuclear Sciences Individual Dosimetry Laboratory.

The TLD placed on the inner surface of the mask and irradiated during treatment of the patient were read by following the steps of TLD reading procedure such as the one during calibration. Following the reading procedure, the dosimeters were annealed in the PTW TLDO oven to make them ready for reuse.

3.2.3 Comparison of calculated doses with measured doses

The calculated doses were recorded on the computer after reading at the determined points. Measured doses were also recorded on computer after the dosimeters were read. Three measurements were recorded for each point marked on the mask. The mean value of these three measurements was calculated and taken as the measured dose value for that point. The calculated doses and measured doses were recorded in a single file and compared. The difference of doses was calculated as percentage using Equation 3.1.

$$\% \text{ difference} = \frac{\text{Measured Dose} - \text{Calculated Dose}}{\text{Calculated Dose}} \quad \text{Equation 3.1}$$

3.2.4 Statistical analysis

SPSS program 25th version was used for statistical evaluations. Following the Alderson Darling Normality test, the paired sample test was used for the comparison. Paired sample test is used to compare a mean of two quantities, situations like before and after or presence or absence of something.

4. RESULTS

Two female and eight male patients were included in the study. Patients were between 20 and 85 years of age. Patients were informed prior to treatment and their approval was taken before their masks were marked. The measured doses were compared with the calculated doses. The skin doses were compared from the 40 points on ten patients. The prescribed dose information for the treatment of patients are given in Table 4.1.

Table 4.1 Treatment Plan Data of the Patients

Patient Number	Daily Dose (cGy)	Number of Fraction (Day)	Total Dose (cGy)
1	212	33	6960
2	212	33	6960
3	200	30	6000
4	180	25	4500
5	212	33	6960
6	180	40	7200
7	200	33	6600
8	212	33	6960
9	212	33	6960
10	200	30	6000

After the treatment plans of the patients were prepared, the mean values of the doses absorbed by the predefined volumes in the planning system were recorded. The calculated dose values and gantry positions are given in Table 4.2.

Table 4.2 Calculated Doses of Determined Volumes

Patient Number	Marked Point		Calculated Doses (cGy)
	Number	Angle	
1	1	80°	92.7
	2	40°	81.8
	3	320°	71.3
	4	280°	89.4
2	1	80°	177.3
	2	40°	183.7
	3	320°	143.5
	4	280°	122.4
3	1	80°	133.3
	2	40°	153.7
	3	320°	180.1
	4	280°	148.4
4	1	80°	161.5
	2	40°	154.9
	3	320°	158.6
	4	280°	155.2
5	1	60°	114.0
	2	20°	119.6
	3	340°	114.5
	4	300°	119.6
6	1	80°	137.1
	2	40°	127.1
	3	320°	126.7
	4	280°	124.2

Table 4.2 Calculated Doses of Determined Volumes (Continued)

7	1	80°	126.1
	2	40°	189.2
	3	320°	171.5
	4	280°	123.9
8	1	60°	133.9
	2	20°	140.2
	3	340°	140.3
	4	300°	147.9
9	1	80°	151.1
	2	40°	143.1
	3	320°	163.6
	4	280°	101.3
10	1	80°	119.0
	2	40°	128.6
	3	320°	106.3
	4	280°	110.1

Skin doses were measured with TLD dosimeters in the first days of treatment. Measurements were taken at the same point for three consecutive days. The mean values of these measurements were calculated. For each patient, four points on the mask were marked, numbered and TLD were placed under masks at these points. Each point has a number which indicates the gantry location where the point was marked. The numbers of the points determined for the measurement, gantry angles, daily measurement results and average values are given in Table 4.3 .

Table 4.3 Measurement Results of TLD Located Under the Mask

Patient Number	Marked Point		Measurement Results (cGy)			
	Number	Angle	Day 1	Day 2	Day 3	Mean Dose (cGy)
1	1	80°	113.2	106.3	114.0	111.2 ± 3.4
	2	40°	90.6	94.5	86.5	90.6 ± 3.2
	3	320°	64.8	86.5	63.2	71.5 ± 10.6
	4	280°	93.5	98.8	91.3	94.6 ± 3.1
2	1	80°	219.4	212.8	212.9	215.1 ± 3.1
	2	40°	188.5	174.7	212.9	192.1 ± 15.8
	3	320°	157.0	158.6	176.4	164.0 ± 8.8
	4	280°	148.5	149.2	136.2	144.7 ± 6.0
3	1	80°	156.8	184.8	161.1	167.6 ± 12.3
	2	40°	163.2	196.4	165.5	175.1 ± 15.2
	3	320°	200.0	210.9	204.6	205.2 ± 4.5
	4	280°	164.7	163.9	162.1	163.6 ± 1.1
4	1	80°	185.5	152.8	173.6	170.7 ± 13.5
	2	40°	157.3	163.1	148.3	156.3 ± 6.1
	3	320°	173.6	175.8	151.5	167.1 ± 10.9
	4	280°	165.4	152.7	161.5	159.9 ± 5.3
5	1	60°	118.6	116.3	111.4	115.4 ± 3.0
	2	20°	138.9	130.8	137.5	135.8 ± 3.5
	3	340°	128.2	128.0	133.1	129.8 ± 2.4
	4	300°	143.2	124.6	158.2	142.01 ± 13.7
6	1	80°	131.8	169.4	142.2	147.9 ± 15.9
	2	40°	164.0	154.2	147.1	155.1 ± 6.9
	3	320°	132.6	134.0	140.8	135.8 ± 3.6
	4	280°	135.0	109.8	141.3	128.7 ± 13.6

Table 4.3 Measurement Results of TLD Located Under the Mask (Continued)

7	1	80°	174.2	166.0	145.7	162.0 ± 11.9
	2	40°	176.2	187.8	227.5	197.2 ± 21.9
	3	320°	191.9	165.0	196.6	184.5 ± 13.9
	4	280°	122.1	146.1	159.4	142.6 ± 15.4
8	1	60°	145.5	152.2	162.3	153.4 ± 6.9
	2	20°	172.9	167.2	173.1	171.1 ± 2.7
	3	340°	170.3	187.6	186.2	181.4 ± 7.8
	4	300°	173.9	175.8	165.4	171.8 ± 4.6
9	1	80°	144.9	156.8	151.9	151.2 ± 4.9
	2	40°	165.4	166.1	176.9	169.5 ± 5.3
	3	320°	192.4	193.3	191.1	192.3 ± 0.9
	4	280°	113.6	99.5	117.8	110.4 ± 7.8
10	1	80°	126.0	142.2	123.2	130.5 ± 8.3
	2	40°	128.6	150.0	122.7	133.8 ± 11.7
	3	320°	121.9	130.0	123.5	125.2 ± 3.5
	4	280°	141.1	144.0	140.8	142.0 ± 1.5

The mean dose of the three-day measurement at a point, was accepted as the absorbed daily dose of that point. The comparison of the mean doses of the measurement results with the calculated dose results are given in the Table 4.4.

Table 4.4 Comparison of Measured and Calculated Doses

Patient Number	Point number	Measured Doses (cGy)	Calculated Doses (cGy)	Difference (cGy)	Difference (%)
1	1	111.2	92.7	18.5	20.0
	2	90.6	81.8	8.8	10.8
	3	71.5	71.3	0.2	0.3
	4	94.6	89.4	5.2	5.8
2	1	215.1	177.3	37.8	21.3
	2	192.1	183.7	8.4	4.6
	3	164.0	143.5	20.5	14.3
	4	144.7	122.4	22.3	18.2
3	1	167.6	133.3	34.3	25.7
	2	175.1	153.7	21.4	13.9
	3	205.2	180.1	25.1	13.9
	4	163.6	148.4	15.2	10.2
4	1	170.7	161.5	9.2	5.7
	2	156.3	154.9	1.4	0.9
	3	167.1	158.6	8.5	5.4
	4	159.9	155.2	4.7	3.0
5	1	115.4	114.0	1.4	1.2
	2	135.8	119.6	16.2	13.5
	3	129.8	114.5	15.3	13.4
	4	142.1	119.6	22.5	18.8
6	1	147.9	137.1	10.8	7.9
	2	155.1	127.1	28.0	22.0
	3	135.8	126.7	9.1	7.2
	4	128.7	124.2	4.5	3.6

Table 4.4 Comparison of Measured and Calculated Doses (Continued)

7	1	162.0	126.1	35.9	28.5
	2	197.2	189.2	8.0	4.2
	3	184.5	171.5	13.0	7.6
	4	142.6	123.9	18.7	15.1
8	1	153.4	133.9	19.5	14.6
	2	171.1	140.2	30.9	22.0
	3	181.4	140.3	41.1	29.3
	4	171.8	147.9	23.9	16.2
9	1	151.2	151.1	0.1	0.1
	2	169.5	143.1	26.4	18.4
	3	192.3	163.6	28.7	17.5
	4	110.4	101.3	9.1	9.0
10	1	130.5	119.0	11.5	9.7
	2	133.8	128.6	5.2	4.0
	3	125.2	106.3	18.9	17.8
	4	142.0	110.1	31.9	29.0

Minimum 0.1cGy and maximum 41.1cGy dose difference was observed when the calculated doses and the measured doses were compared. When the results are examined as percentage the difference between measured doses and calculated doses are ranged from minimum 0.1% to maximum 29.3%.

While measurement results and calculation results were evaluated statistically, Alderson Darling Normality test and Paired Sample t test were applied. Statistical comparison is given in Table 4.5.

Table 4.5 Paired Sample Test Statistics

Dose Value	Mean Dose (cGy)	N (number of samples)	Standard Deviation	P < 0.001
Calculated	134.6	40	27.7	
Measured	151.4	40	31.4	

According to comparison of 40 points an average of 12.6 % difference was observed between calculated and measured doses. Measured doses are higher than the calculated doses at all points. The differences between the measurement results and the calculation results were statistically significant ($p < 0.001$). This means the probability of the calculated and the measured doses to have randomly same value is less than 0.1%. This result supported that the doses caused by the masks are not calculated correctly by the TPS.

The total absorbed doses by the four determined points for each patient were calculated and averaged for both calculated results and measured results. Figure 4.1 shows the comparison of the mean values for each patient.

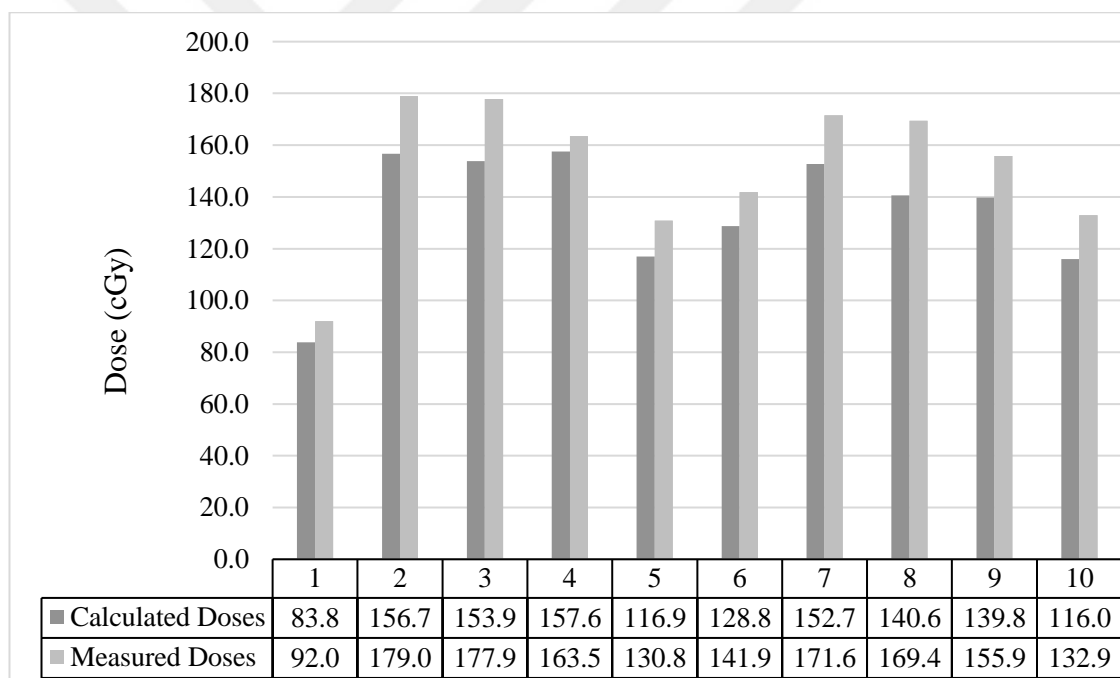


Figure 4.1 Mean of Calculated and Measured Skin Dose Values for each Patient

As can be seen from figure 4.1 the mean of measured doses of four point for each patient are higher than the calculated mean dose of four points. While the smallest difference is 3.7 % (patient 4), the highest difference 20.5% (patient 8).

5. DISCUSSION

In the study, the average daily dose calculated of the forty points by the planning system was 134.6 cGy while the daily dose measured by TLD was 151.4 cGy. The average difference of 16.8 cGy which was not calculated by the planning system corresponds to a percentage of 12.6%. The lowest difference between the measured values and calculated values is 0.1% and the highest difference is 29.3%. Measured doses were higher than calculated doses. According to this comparison, the difference between the calculated doses and the measured doses was statistically significant ($p < 0.001$).

The dose difference with the lowest percentage in our study is 0,1 cGy and dose difference with the highest percentage is 41.1 cGy . When these doses are multiplied with treatment fractions, the total dose differences are ranging between 3.3 cGy to 1350 cGy. In other words the patient skin absorbs up to 1350 cGy higher radiation dose than expected. Doses in these amounts may lead to serious increase in skin toxicity.

As the inadequacy of TPS to calculate skin doses is known, skin doses are measured and compared with the planning system calculation results in many clinics. For example, in a study by Court et al., the surface doses were measured with MOSFET detectors, during the irradiation of a phantom by using the IMRT plan generated in the Eclipse TPS. The results were compared with the surface doses calculated by the Eclipse planning system. They compared the measured doses with mean doses absorbed by the volumes at a depth of 2mm of the skin contour. The difference in results was less than 10% in 75% of the results and less than 20% in 94% (Court et al. 2007). However, when the results of this study was examined, the difference between the measurements and the calculations was less than 10% in 42.5% of all points and the difference is 20% in 82.5%. Eclipse TPS version 10.0.0 was being used in the study to create IMRT plans. This was the same planning system and the same version with the one used in this study. In addition, this study was similar to the present study in terms of the plans used which were IMRT plans. However, in the study of Court et al. (2007), thermoplastic mask was not used. When the mask usage and the higher results of our study was considered, the difference between two studies can be attributed to the effect of the thermoplastic mask. However, there are

a number of factors that can cause differences in the measured and calculated doses apart from the mask. For example, while the measurements in this study were taken on the patient in vivo, a phantom was used in the study of Court et al. (2007). This may cause differences due to setup errors. However, this difference will be negligible as the measurements were made in the first days of the treatment so that there was no distance between the patient skin and the mask and in the positions verified by the EPID image.

A similar study was conducted by Zhuang and Olch (2014). In their study, they scanned the pelvic phantom in CT and created IMRT plans via the Eclipse planning system. They irradiated the pelvic phantom with IMRT plans and measured the skin doses with diode and OSL dosimeters. They compared the results of measurement and calculations. They read the calculated values at a depth of 1 mm of the body contour. The results of OSL dosimeters and the doses calculated by the planning system showed a difference of 1.7% to 2.2% according to the data of two points. However, according to the results of the diode dosimeter measurements, up to 10.1% difference was observed (Zhuang and Olch 2014). Thermoplastic mask was not used in Zhuang and Olch's work. When the results of the study was investigated, it was seen that the difference between the two dosimeters and the planning system were high. One of the reasons for this was that the scattering doses cannot be adequately calculated by the planning system due to the thermoplastic mask, and another cause may be due to setup errors. However, as mentioned before, setup errors in this study were very small and negligible because the measurements were recorded in the first days of the patient treatment and the patient position was confirmed by EPID dosimetry.

One of the differences between the three studies; namely, this study, Zhuang and Olch's study and Court et al.'s study, may be due to the fact that different dosimeters were used in each study. However, in one study, the measured skin dose was considered to be the measured value, regardless of the type of dosimeter used (Court et al. 2007). TLD was the dosimeter that can cause the most error among the dosimeters used (Kinhikar et al. 2009). In the present study, the dosimeters which deviated more than 5% during calibration were excluded and the mean deviation dropped to 4%. Even if this deviation was considered, the difference between the measurements and the calculated values was higher than the results of the two other studies which were performed without the

thermoplastic masks. Therefore, the difference between the calculated doses in the planning system and the doses measured in vivo can be thought to be mask-induced.

A similar study was carried out by Qi et al. (2008), by using a different type of linear accelerator called “tomotherapy” and its planning system CORVUS software. They created IMRT plans for head and neck cancer patients with thermoplastic masks. They measured the skin doses on 16 points from six patients using MOSFET detector during the treatment. They compared the calculation results with the measurements. They found that the calculated doses were higher than measured doses in the range of 4.3% to 9.2%, an average of 7.2% (Qi et al. 2008).

Kinhikar et al. (2009) performed a similar study using the tomotherapy device and the Tomoplan TPS version 2.2. They measured skin doses in two head and neck patient under mask, using TLD and MOSFET. For the first patient the doses were measured as 92% and 90% with TLD and MOSFET, respectively, while the calculated dose was 100%. For the second patient the doses were measured as 86% and 88% with TLD and MOSFET respectively, while the calculated was 100% again. In other words, the calculated doses are 8-14% higher than in vivo measured doses (Kinhikar et al. 2009).

There was a main difference between the results of these two studies and the present study. The measured doses are lower than the calculated doses in these two studies, in contrast to this study. The planning system used at these studies included the scattering of masks but could not find a coherent result. It overestimated the effect of the mask. Over estimation of the skin doses may cause the skin to absorb less dose than desired, when the target is skin or fields close to skin.

Even if their methods are different, there are many studies showing the effect of thermoplastic masks on skin dose. For instance, Fiorino et al. (1994) performed an in vitro study on three different undeflected masks and showed that the masks increased the surface dose in the range between %30 and %62. Soleymanifard et al. (2014) examined the vertical and tangential beams in a rando phantom and two different thermoplastic masks with TLD. In the case of 6 MeV X-ray usage the surface dose was measured for vertical and for tangential beams and it was found that the dose increase due to thermoplastic mask was 38% and 22% for vertical and tangential beams, respectively (Soleymanifard et al. 2014).

The mask pattern, perforation frequency and thickness of the mask directly effects the dose increase in the surface (Fiorino et al. 1994). According to Hadley et al. (2005) the masks increased the surface doses up to 62%. The mask with small holes caused up to 61% increase at the surface dose and the masks with the large holes caused up to %52 increase at the surface dose when 6MV X-rays were applied (Hadley et al. 2005). According to Lee et al. (2002)'s study on rando phantom, 18% average increase in surface doses was found when the thermoplastic mask was applied. (Lee et al 2002).

When this study was analyzed from this perspective, the difference between the calculated doses and the measured doses remained below the dose increase of the masks in other studies. However, this may be caused by the fact that the masks used in the studies were not stretched masks. The results of the present study were very close to the results of Lee et al. (2002) as stretched mask is used in the measurements. Also the TLD location may affect the results if it is placed under mask or placed in perforation. It would not be wrong to say that an average of 12.6% difference can be caused by the mask.

6. CONCLUSION AND RECOMMENDATION

During radiation treatment period, side effects are expected for the skin. During head and neck radiation treatment, five to seven weeks, severe toxicities due to radiotherapy in the skin of the area receiving radiotherapy can be seen (Bahl et al. 2012, Snider et al. 2015). Thermoplastic masks used for immobilization of the head and neck region are the structures that cause interactions with the radiation coming to the patient and cause scattering which results in undesired dose increase in the patient's skin. This may lead to an increase in the patient's skin toxicity. Therefore, the amount of dose to be absorbed by the patient's skin should be accurately estimated and appropriate treatment recommendations should be made for the side effects that may occur on the patient. However, TPS are insufficient to calculate input doses. In addition, when the thermoplastic material is included in the calculation, they cannot accurately calculate the mask doses due to scattering and back scattering of these structures (Qi et al. 2008, Court et al. 2007).

The aim of this study was to evaluate the accuracy of the calculated skin doses and find the effect of the thermoplastic mask which can not be calculated by the planning system. In this study, the daily doses calculated from the determined points in the planning system and the daily doses obtained by in vivo measurement of these points were compared. In order to prevent weight loss-related changes and setup errors, measurements were taken on the first days of the treatment of the patient. Skin dose measurements were performed for three consecutive days with TLD placed on the inner surface of the thermoplastic mask during treatment. Skin doses were also read from the TPS, under the skin contour. When creating the skin contour, the thermoplastic mask is automatically left out of the contour.

The results obtained from the patients were compared with the doses prescribed by the TPS. The difference was evaluated as the mask effect which could not be calculated by the planning system.

In conclusion, there were serious and significant differences between calculated doses and measured doses in our study. According to these differences, the effect of

thermoplastic masks could not be accurately calculated by the planning system. With the effect of the mask, it has been observed that more radiation was absorbed by the skin, than expected. Considering its usefulness and necessity, it is not possible to discontinue the use of thermoplastic masks. Because TPS are inadequate in calculating skin doses, it is important to measure skin doses under the mask clinically. Moreover, since the physical condition of the patients using the mask affects the thickness of the mask and the size of the holes, it is not correct to estimate a general dose for each patient with a single mask measurement. This emphasizes the importance of performing in-vivo measurements under the mask to estimate the doses that the patient will take.

Our study was performed on patients who did not receive the same doses and who have different diagnoses. For future studies, measuring skin dose in patients with the same dose and increased patient size may lead to more accurate statistical results. A similar study can be performed by scanning a phantom by CT with mask and without mask, and by creating treatment plans on the planning system in both groups. Thus, this will show the amount and percentage of error due to mask-related doses.

In this study, the importance of accurate calculation of the effect of thermoplastic mask and in vivo measurements were emphasized in order to recommend appropriate treatments for the expected reactions in the skin for patients receiving head and neck radiotherapy.

REFERENCES

- Aboud, H., Wagiran, H., Hussin, R. 2012. Mechanism of Thermoluminescence. *International Journal of Scientific & Engineering Research*, 3 (10); 650-665.
- Babic, S., Jordan, K. 2012. The performance of an optical cone-beam CT scanner adapted for radiochromic film dosimetry. *Physics in Medicine and Biology*, 57 (2012); N377 - N389.
- Bahl, A., Ghosal, S., Kapoor, R., Bhattacharya, T., Sharma, S. C. 2012. Clinical Implications of Thermoplastic mask Immobilization on Acute Effects of Radiotherapy in Head and Neck Cancers. *Journal of Postgraduate Medicine Education and Research*, 46 (4); 187 – 189.
- Baldock, C., De Deene, Y., Doran, S., Ibbott, G., Jirasek, A., Lepage, M., McAuley K. B., Oldham, M., Schreiner, L. J. 2010. Topical Review: Polymer gel dosimetry. *Physics in Medicine and Biology*, 55 (5); R1 – R63.
- Blessing Cathay Corporation. 2018. Web site. http://www.bcc.taipei/RTproducts/product_timokit.html Last Accessed: 10 December 2018.
- Bos, A. J. J. 2007. Theory of thermoluminescence. *Radiation Measurements*, 41 (1); S45 –S56
- Canadian Nuclear Safety Commission. 2011. Introduction to Dosimetry INFO 0827, Minister of Public Works and Government Services Canada.
- Court, L. E., Tishler, R. B., Allen, A. M., Xiang, H., Makrigrigios, M., Chin, L. 2007. Experimental evaluation of the accuracy of skin dose calculation for a commercial treatment planning system. *Journal of Applied Clinical Medical Physics*, 9 (1); 29 – 35.
- Çetingöz, R. 2013. Temel ve Klinik Radyoterapi. *Türk Radasyon Onkolojisi Derneği (TROD) Yayınları*, p.173 - 207, İzmir.
- Engin, K., Erişen, L. 2003. Baş- Boyun Kanseri. *Nobel Tıp Kitabevleri*, p. 33-296, Bursa.
- Evwierhurma, O. B., Ibitoye, Z.A., Ojeh, C. A., Duncan J. 2015. Verification of entrance dose measurements with thermoluminescence dosimeters in conventional radiotherapy procedures delivered with Co-60 Teletherapy Machine. *Annals of Medical & Health Sciences Research*, 5 (6); 409 - 412.
- Fiorino, C., Cattaneo G. M., Vecchio, A. D., Longobardi, B., Signorotto, P., Calandrino, R., Fosatti, V., Volterrani, F. 1992. Skin dose measurement for head and neck radiotherapy. *Medical Physics*, 19(5); 1263-1266.
- Fiorino, C., Cattaneo, G. M., Vecchio, A. D., Fusca, M., Longobardi, B., Signorotto, P., Calandrino, R. 1994. Skin-sparing reduction effects of thermoplastics used for patient immobilization in head and neck radiotherapy. *Radiotherapy and Oncology*, 30 (3); 267 – 270.

- Furetta, C. 2003. Handbook of Thermoluminescence. World Scientific Publishing Co. Pte. Ltd., p.148 - 326, Singapore.
- Galbiatti, A. L. S., Padovani-Junior, J.A., Maniglia, J. V., Rodrigues, C. D. S., Pavarino, E. C., Bertollo, E. M. G. 2013. Head and Neck Cancers Causes, Prevention and Treatment. Brazilian Journal of Otorhinolaryngology (BJORL), 79(2), 239-247.
- Gear, J. I., Charles-Edwards, E., Partridge, M., Flux, G. D. 2011. Monte Carlo verification of polymer gel dosimetry applied to radionuclide therapy: a phantom study. Physics in Medicine and Biology, 56 (2011); 7273 – 7286.
- Gundersen, L. L., Tepper, J. E. 2016. Clinical Radiation Oncology. Elsevier Incorporation, p.276-564, Philadelphia.
- Gupta, B., Johnson, N. W., Kumar, N. 2016. Global Epidemiology of Head and Neck Cancers: A continuing Challenge, Oncology, 91(1); 13-23.
- Hadley, S. W., Kelly, R., Lam, K. 2005. Effects of immobilization mask material on surface dose. Journal of Applied Clinical Medical Physics, 6(1); 1- 7.
- Halk Sağlığı Genel Müdürlüğü. 2017. Web site. <http://kanser.gov.tr/index.php/kanser/kanser-turleri/774-ba%C5%9F-ve-boyun-kanserleri> Last Accessed: 27 April 2018.
- Haridas, G. N., Dev, V., Nayak, M. K., Thakkar, K. K., Sarkar, P. K., Sharma, D. N. 2006. Determination of dose buildup thickness for absorbed dose measurement in high energy electron-photon radiation at electron storage rings. Radiation Protection Dosimetry, 121 (2); 92-98.
- International Atomic Energy Agency. 2013. Developments of Procedures for In Vivo Dosimetry in Radiotherapy, IAEA Human Health Reports No 8, Vienna.
- International Commission on Radiation Units and Measurements. 2010. Prescribing, Recording and Reporting Photon Beam Therapy, ICRU Report 83, Glasgow.
- Jesper, C., Vestergaard, A. 2000. Skin damage probabilities using fixation materials in high – energy photon beams. Radiotherapy and Oncology, 55(2000); 191-198.
- Khan, F. M. 2014. The Physics of Radiation Therapy fifth edition. Lippincott Williams & Wilkins, p.121-445, Philadelphia.
- Ki-Oh, K., Lim, C.H., Hyun, L.D., Jung, H. R., Park, M. J., Lee, J. Y. 2016. A Study on Skin Dose Changes in Body Weight from Tomotherapy for Head and Neck Cancer. Indian Journal of Science and Technology, 9(25), 1-5.
- Kinhikar, R. A., Murthy, V., Goel, V., Tambe, C. M., Dhote, D. S., Deshpande, D. D. 2009 Skin dose measurements using MOSFET and TLD for head and neck patients treated with tomotherapy. Applied Radiation and Isotopes, 67(9); 1683-685.
- Kwan, I. S., Rosenfeld, A. B., Qi, Z. Y., Wilkinson, D., Lerch, M. L. F., Cutajar, D. L., Safavi-Naeni, M., Buston, M., Bucci, J. A., Chin, Y., Perevertaylo, V. L. 2008. Skin dosimetry with new MOSFET detectors. Radiation Measurement, 46 (2- 6); 929- 932.

- Lee, N., Chuang, C., Quivey, J. M., Philips, T. L., Akazawa, P., Verhey, L. J., Xia, P. 2002. Skin toxicity due to intensity-modulated radiotherapy for head and neck carcinoma. *International Journal of Radiation Oncology *biology *physics*, 53 (3); 630-637.
- Lester, S., Young, Y. W. 2012. Principles and Management of Head and Neck Cancer. *Surgery*, 30 (11); 617- 623.
- Medical Expo. 2018. Web Site. <http://www.medicaexpo.com/prod/varianoncology/product-70440-424098.html> Last Accessed: 10 December 2018.
- Mellenberg, D. E. 1995. Dose behind various immobilization and beam modifying devices. *International Journal of Radiation Oncology Biology Physics*, 32(4); 1193- 1197.
- Mijnheer, B., Beddar, S., Izewska, J., Reft, C. 2013. In vivo dosimetry in external beam radiotherapy. *Medical Physics*, 40(7); 070903.
- My Radiotherapy. 2010. Web Site: http://www.myradiotherapy.com/general/treatment/Treatment_Machines/diodes/Diodes.html Last Accessed. 10 December 2018.
- Nasage Landauer LTD. 2018. Web Site. <https://www.nagase-landauer.co.jp/english/inlight/technology.html> Last Accessed: 10 December 2018.
- Nishimura, Y., Komaki, R. 2015. Intensity Modulated Radiation Therapy Clinical Evidence and Techniques. Springer Japan, 5, Japan.
- Perez, C. A., Brandy, L. W. 2013. Principles and Practice of Radiation Oncology. Lippincott Williams & Wilkins, 402- 403, Philadelphia.
- Podgorsak, E. B. 2010. Radiation Physics for Medical Physicists, Springer p. 84- 310 Heidelberg.
- Poltorak, M., Fujak, E., Kukolowicz, P. 2016. Effect of the thermoplastic masks on dose distribution in the build-up region for photon beams. *Polish Journal of Medical Physics and Engineering*, 22(1); 1-4.
- Qi, Z.Y., Deng, X. W., Huang, S. M., Zhang, L., He, Z. C., Li, X. A., Kwan, A. L., Lerch, M., Cutajar, D., Metcalfe, P., Rosenfeld, A. 2008. In vivo verification of superficial dose for head and neck treatments using intensity-modulated techniques. *Medical Physics*, 36 (1); 59 – 70.
- RADAT Dozimetri Laboratuvar Hizmetleri A.Ş. 2018. Web Site. <https://www.radat.com.tr/documents/tld-oven.pdf> Last Accessed: 10 December 2018.
- Rensselaer Polytechnic Institute. 2018. Web Site. http://www.rpi.edu/dept/radsafe/public_html/instruments.html Last Accessed: 27 April 2018.
- Sanderson, R. J., Ironside, J. A. D. Squamous cell carcinomas of head and neck. *The British Medical Journal*, 325(7368); 822-827.
- Snider, J. W., Kalavagunta, C., Xu, H., Schrum, A., Vadnais, P., Marter, K., Lin, M. H., Suntharalingam, M. 2015. Bolus Effect of Immobilization Masks in Head and Neck Radiation Therapy Mitigated by Mask Alteration and Dosimetric

Optimization for Skin Avoidance. *International Journal of Radiation Oncology Biology Physics*, 93 (3); 627 – 628.

Soleymanifard, S., Toossi, M. T. B., Khosroabadi, M., Noghreiyani, A. V., Shahidsales, S., Tabrizi, F. V. 2014. Assessment of skin dose modification caused by application of immobilizing cast in head and neck radiotherapy. *Australasian Physical & engineering sciences in medicine*, 37(3); 535 – 540.

Tariq, A., Mehmood, Y., Jamshaid, M., Yousaf, H. 2015. Head and Neck Cancers: Incidence, Epidemiological Risk and Treatment Options. *International Journal of Pharmaceutical Research & Allied Sciences*, 4(3), 21 -34.

Thermo Fisher Scientific. 2018. Web Site. <https://www.thermofisher.com/order/catalog/product/3500TLDDS3> Last Accessed: 10 December 2018.

Yeh, S. 2010. Radiotherapy for Head and Neck Cancer. *Seminars in Plastic Surgery*, 24(2); 127 - 136.

Yu, P. K. N., Cheung, T., Butson, M. J. 2003. Variations in skin dose using 6MV or 18MV x-ray beams. *Australasian Physical & Engineering Sciences in Medicine*, 26 (2); 79 – 81.

Zhuang, A. H, Olch, A. J. 2014. Validation of OSLD and a treatment system for surface dose determination in IMRT treatments. *Medical Physics*, 41(8); 081720.

CURRICULUM VITAE

Name Surname: Elçin İlke Okur

Birth Place: Eskişehir

Birth Date: 20. 06. 1989

Marital Status: Single

Languages: Turkish, English

Educational Information: High School: Bilecik Refik Arslan Öztürk Science High School 2007

Bachelors Degree: Hacettepe University Nuclear Energy Engineering 2014

Master of Science: Ankara University Institute of Nuclear Sciences Medical Physics

Department, Health Physics Program 2019